LAWRENCE
LIVERMORE
NATIONAL
LABORATORY

UCRL-TR-227386

DYNA3D Finite Element Analysis of Steam Explosion Loads on a Pedestal Wall Design

C. R. Noble

January 22, 2007

This work was performed under the auspices of the U.S. Department of Energy by University of California, Lawrence Livermore National Laboratory under Contract W-7405-Eng-48.

DYNA3D Finite Element Analysis of Steam Explosion Loads on a Pedestal Wall Design

Charles R. Noble

January 16, 2007

This work was performed under the auspices of the U.S. Department of Energy by the University of California, Lawrence Livermore National Laboratory under contract No. W-7405-Eng-48.

1.0 Objective

The objective of this brief report is to document the ESBWR pedestal wall finite element analyses that were performed as a quick turnaround effort in July 2005 at Lawrence Livermore National Laboratory and describe the assumptions and failure criteria used for these analyses [Ref 4]. The analyses described within are for the pedestal wall design that included an internal steel liner. The goal of the finite element analyses was to assist in determining the load carrying capacity of the ESBWR pedestal wall subjected to an impulsive pressure generated by a steam explosion.

2.0 Model Description

The DYNA3D (ParaDyn) [Ref 2] finite element model used 1/8 symmetry and 523,887 solid hexahedral elements for the concrete and rebar materials, 13,200 shell elements for the liner, and 501,600 nodes. The finite element model is shown in Figure 1. A summary of the material properties assumed for each material at the time of the simulation is presented in Table 1. A kinematic isotropic elastic plastic material model was used for the steel liner and rebar materials and the Karagozian & Case nonlinear constitutive model was used for the concrete. Symmetry boundary conditions were applied to the sides of the finite element domain and the base of the pedestal wall was assumed to be completely fixed in all three global directions.

3.0 Material Model Descriptions and Damage Metrics

3.1 Material Models

The K&C concrete model was developed by Javier Malvar, Jim Wesevich, and John Crawford of Karagozian and Case, and Don Simon of Logicon RDA [Ref 3]. The concrete model uses three independent fixed surfaces to define the plastic behavior of concrete (see Figure 2). The three surfaces are defined by pressure on the horizontal axis and deviatoric

stress on the vertical axis. These three surfaces define three important regions of concrete behavior. It can be seen easily if one plots the stress-strain response for a uniaxial unconfined compression test (see Figure 2). The material response is considered linear up until point 1, or first yield. After yielding, a hardening plasticity response occurs until point 2, or maximum strength, is reached. After reaching a maximum strength, softening occurs until a residual strength, which is based on the amount of concrete confinement, is obtained.

For this analysis, complete concrete damage is defined as concrete which has reached the residual strength of the concrete material. The post-processor will use the color red to denote concrete which has reached point 3 (Figure 2). Furthermore, this concrete material model takes into account strain-rate enhancement. At high strain rates, the apparent strength of concrete and the corresponding strain at peak stress both increase. It has been shown by experimental tests that there are different rate enhancements for tensile and compressive loading. The strain rate enhancement factors used are those determined by the Air Force and are shown in Figure 3. For a more detailed discussion on this concrete damage model, please refer to the attached appendix. Extensive verification and validation of this material model has also been performed by Karagozian & Case [Ref 1].

A kinematic isotropic/elastic-plastic material model was used for the steel liner and rebar materials. Material failure for this model is determined in the post-processing step of the analysis and is not modeled within the constitutive model itself. During the post-processing step, material failure may be determined by thresholding the steel effective plastic strain at various values, with a value of 0.2 or 20% being the typical value assumed.

model includes 10 m high by 45 degrees by 2.4 m thick section of reinforced concrete

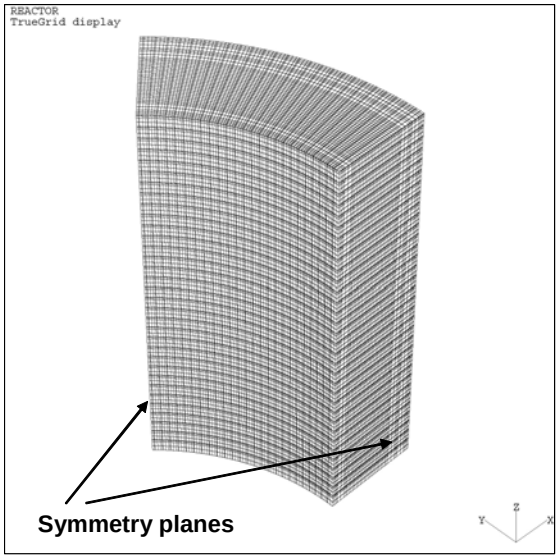

Concrete

f'_c = 5,000 psi

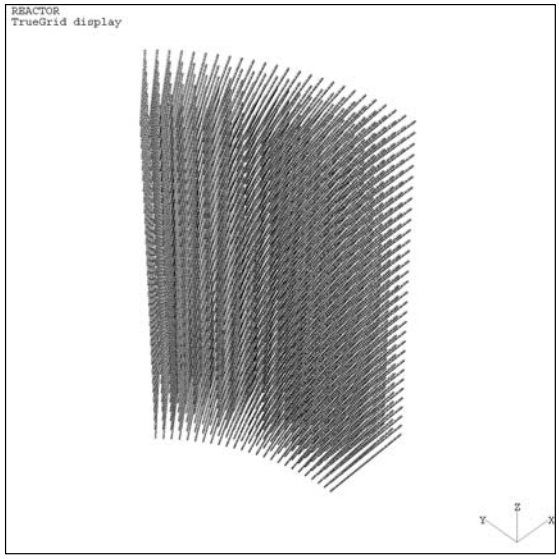

Shear Rebar

σ_y = 60,000 psi

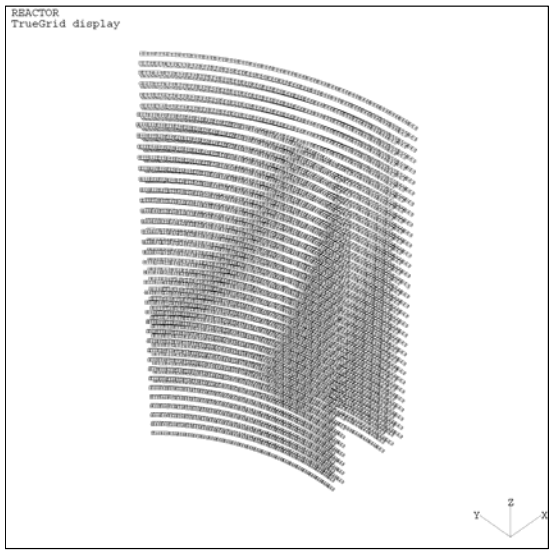

Hoop Rebar

σ_y = 60,000 psi

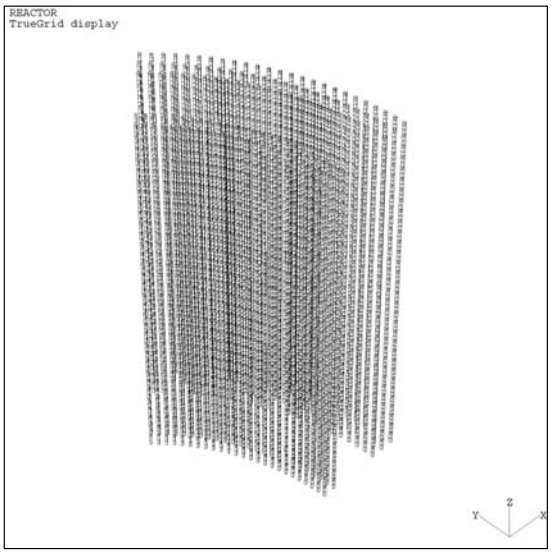

Vertical Rebar

σ_y = 60,000 psi

FIGURE 1. DYNA3D finite element model.

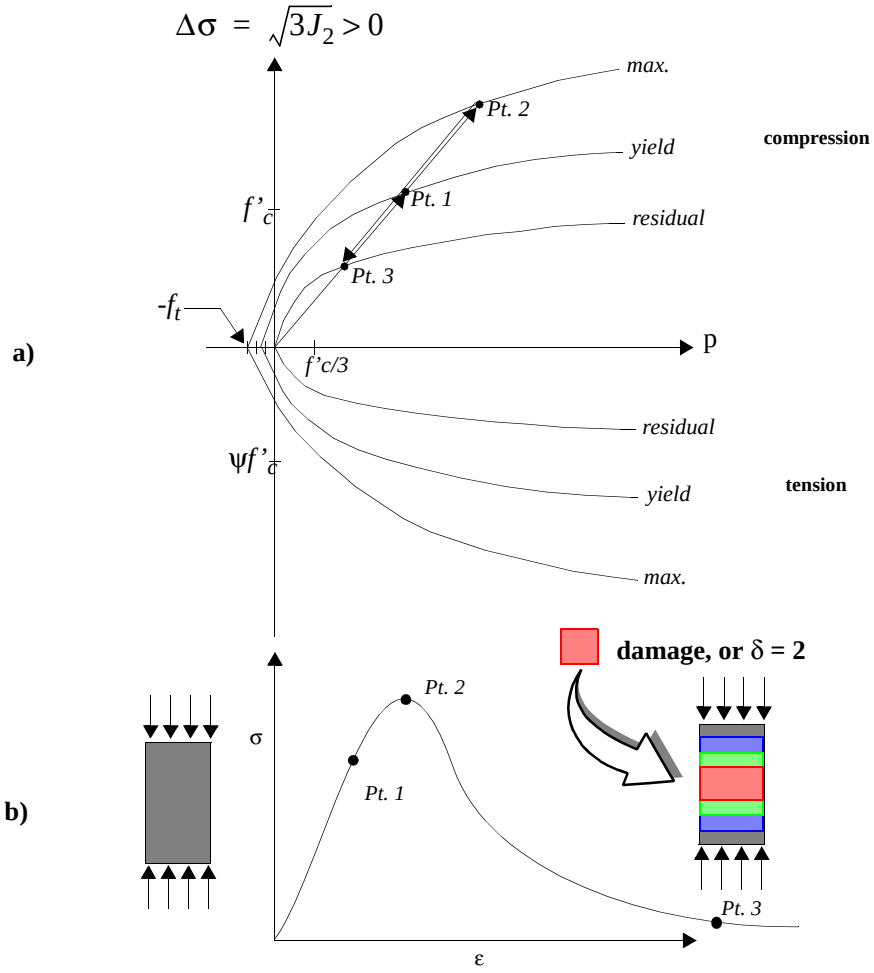

FIGURE 2. a). Three independent fixed failure surfaces for DTRA concrete material model; b). Uniaxial representation of concrete stress-strain curve.

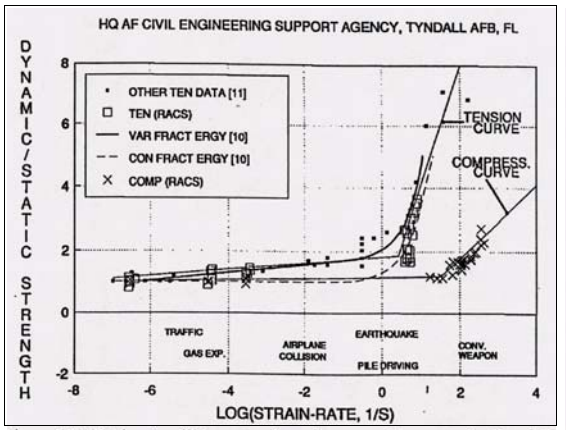

FIGURE 3. Strain rate effects on tensile and compressive strengths determined by Air Force.

TABLE 1. Assumed Finite Element Material Properties

Material Property	Value	Units
Concrete compressive strength	5000	psi
Concrete tensile strength	500	psi
Rebar modulus of elasticity	29e+06	psi
Rebar Poisson's ratio	0.29	
Rebar yield strength	60000	psi
Rebar tangent modulus	110800	psi
Steel liner modulus of elasticity	27.2e+06	psi
Steel liner Poisson's ratio	0.3	
Steel liner yield strength	33140	psi
Steel liner tangent modulus	556000	psi

3.2 Failure Criteria for Pedestal Wall

Multiple criteria was used to determine failure of the pedestal wall. The first criteria was the concrete damage parameter within the Karagozian & Case material model. The damage parameter shows, in a simplified sense, at what location on the stress-strain curve the concrete is at. For example, undamaged concrete or concrete that has not reached first yield, is shown in a blue color. Material that has reached maximum yield is shown in a green color, and material that has reached its residual strength is shown in a red color. Unfortunately, a concrete damage parameter, by itself, is not necessarily a good indicator of structural integrity after an extreme loading event. In other words, a concrete damage criterion, either using an internally calculated "damage parameter" or a shear criterion, does not give the structural analyst an indication of the remaining strength in the other structural members, such as the rebar or the steel liner. Effective plastic strain was the variable used to evaluate the damage to the steel. In the original simulations, it was

assumed that the rebar would fail if the effective plastic strain was 20% or higher. The failure strains for the steel liner was assumed to be a higher value of 30%, due to the ductility that was assumed for this material at the time of the calculation. Total failure of the pedestal wall is assumed to occur if the concrete is fully damaged and the rebar has reached 20% effective plastic strain throughout the entire wall section.

4.0 Simulations

This brief report will discuss only the three simulations that included an internal steel liner. The only difference between the three simulations was the impulse applied to the structure. The pressure time histories used for the three different cases are shown in Figure 4. The three different pressure time histories have three different impulses: approximately 200 KPa-sec, 300 KPa-sec, and 600 KPa-sec. A brief damage summary is presented for all three cases in Table 2.

5.0 200 KPa-sec Case

Figures 5 through 8 show the concrete damage, steel liner effective plastic strain, and rebar effective plastic strain pseudocolor plots for the 200 KPa-sec impulse case at a simulation time of 0.039 seconds. The concrete is significantly damaged at the bottom portion of the pedestal wall. The concrete that is shown in red is at its residual strength and is considered completely damaged, which for this constitutive relationship means that the concrete has some strength based on the amount of confining pressure the concrete is experiencing. If the concrete is not confined and is fully damaged, the concrete has virtually no strength. Therefore, material that is not confined by rebar, such as the cover concrete on the backside of the pedestal wall, is most likely going to spall off of the structure. The steel liner has a peak effective plastic strain value of 9.81% at the base of the structure where the finite element model is fixed. This value is therefore the maximum value shown in the pseudocolor plot legend shown in Figure 6. The maximum rebar effective plastic strain is shown to be 12.89%, which also occurs at the base of the pedestal wall. None of the rebar strains come close to the assumed failure criterion of 20%. The outer hoop rebar strains are shown to have values near 4%, based on the pseudocolor plot shown in Figure 8.

6.0 300 KPa-sec Case

Figures 9 through 12 show the concrete damage, steel liner effective plastic strain, and rebar effective plastic strain pseudocolor plots for the 300 KPa-sec impulse case at a simulation time of 0.038 seconds. The calculation predicts the concrete to be fully damaged at the base of the pedestal wall. To evaluate whether the pedestal wall has been fully ruptured, the rebar strains must be analyzed similar to the 200 KPa-sec case. If the rebar strains are not predicted to be near rebar rupture strain levels, the majority of the damaged concrete may be confined within the rebar cage and total failure of the pedestal wall may not be predicted. A significant amount of the axial rebar at the base of the pedestal wall

has reached the assumed failure strain of 20%. From the pseudocolor plots, however, it appears that the outermost axial rebar has not reached 20% effective plastic strain levels and the outermost hoop rebar is experiencing strain levels near 7%. This can all be seen by closely examining Figure 12. It is therefore predicted that although the concrete is fully damaged throughout the entire bottom section of the wall, the rebar may have some residual strength to provide concrete confinement and prevent total failure of the wall. This simulation predicts peak steel liner strains near 20-24% at the base of the pedestal wall.

7.0 600 KPa-sec Case

Figures 13 through 16 show the concrete damage, steel liner effective plastic strain, and rebar effective plastic strain pseudocolor plots for the 600 KPa-sec impulse case at a simulation time of 0.024 seconds. Again, the concrete is predicted to have extensive damage throughout the base of the pedestal wall. The steel liner effective plastic strains have reached a level of 30% or higher at the base of the pedestal wall and is predicted to rupture. The strain levels have reached 20% or higher for all of the axial rebar at the base of the pedestal wall and is not expected to carry any further load. Significant strains reaching levels near 20% are also predicted for the outermost hoop rebar (shown in Figure 16) and is also not expected to carry any further load. Definite wall failure is predicted for this impulse level.

TABLE 2. Damage summary.

Impulse Level KPa-sec	Concrete Damage at Base	Axial Rebar Strains at Base (EPS)[a]	Hoop Rebar Strains at Base (EPS)	Liner Strains at Base (EPS)
200	Fully Damaged	12.89%	4%	9.81%
300	Fully Damaged	Outermost rebar has not reached 20% strain levels	7%	20-24%
600	Fully Damaged	20% or higher	20% or higher	30% or higher

a. Effective Plastic Strain

8.0 References

1. Crawford, J.E., L.J. Malvar, Shi, Y. Verification and Validation for DYNA3D Models of RC Components Subjected to Cased and Uncased Munitions. Karagozian & Case, TR-99-10.3, October 26, 2004.
2. Lin, J., DYNA3D: A Nonlinear, Explicit, Three-Dimensional Finite Element Code for Solid and Structural Mechanics User's Manual, UCRL-MA-107254, January 2005.
3. Malvar, L.J., Crawford, J.E., Wesevich, J.W., Simons, D. A Plasticity Concrete Material Model for DYNA3D. Int. J. Impact Engng, Vol. 19, Nos. 9-10, pp. 847-873, 1997.

4. Noble, C.R. Finite Element Analysis of Nuclear Reactor Components. Lawrence Livermore National Laboratory, UCRL-PRES-214986, August 1, 2005.

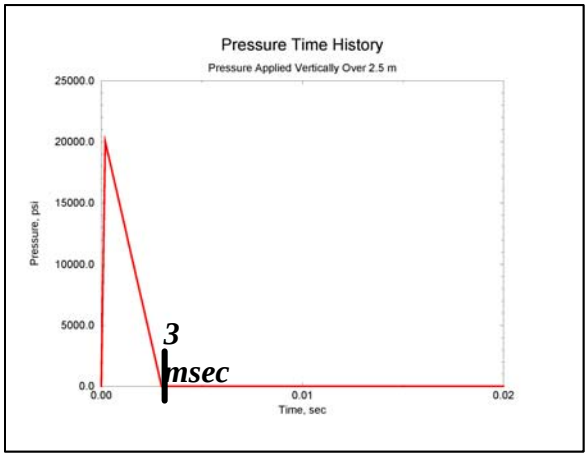

200 KPa-s

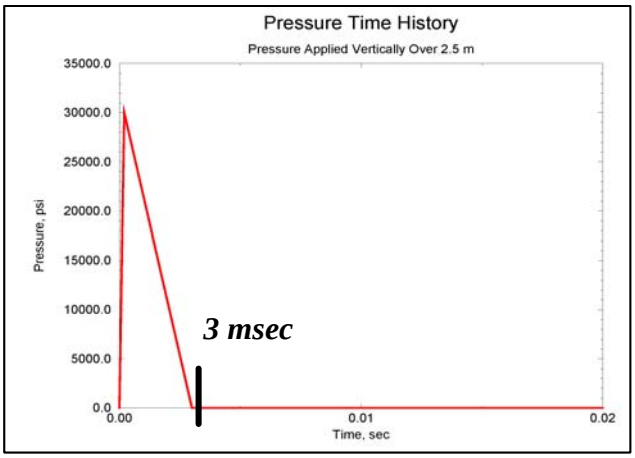

300 KPa-s

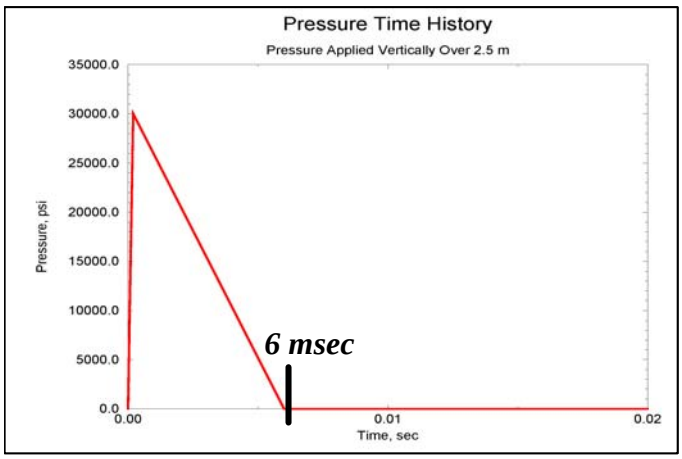

600 KPa-s

FIGURE 4. Pressure time histories applied to structure.

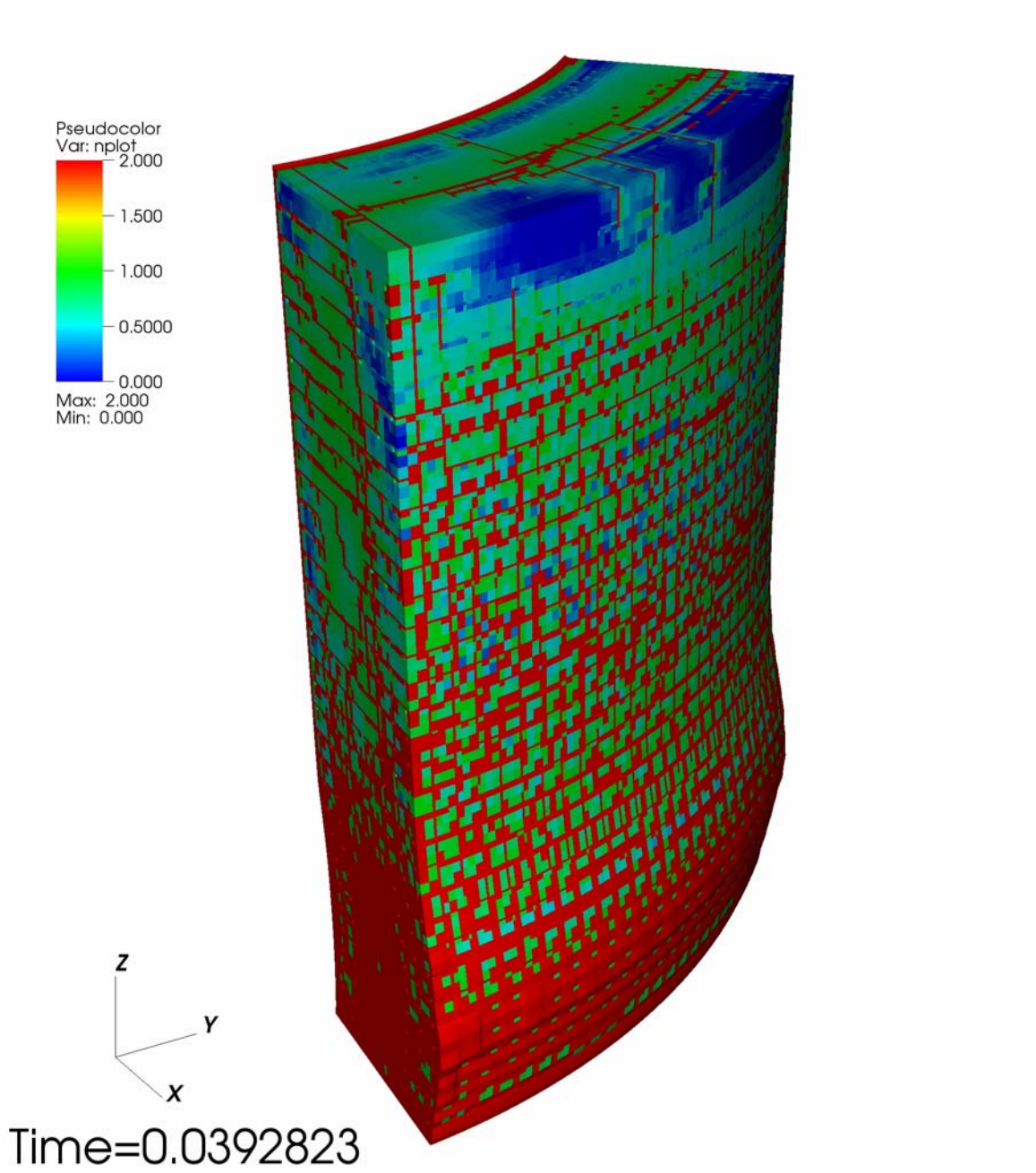

FIGURE 5. Concrete damage pseudocolor plot for 200 KPa-sec case.

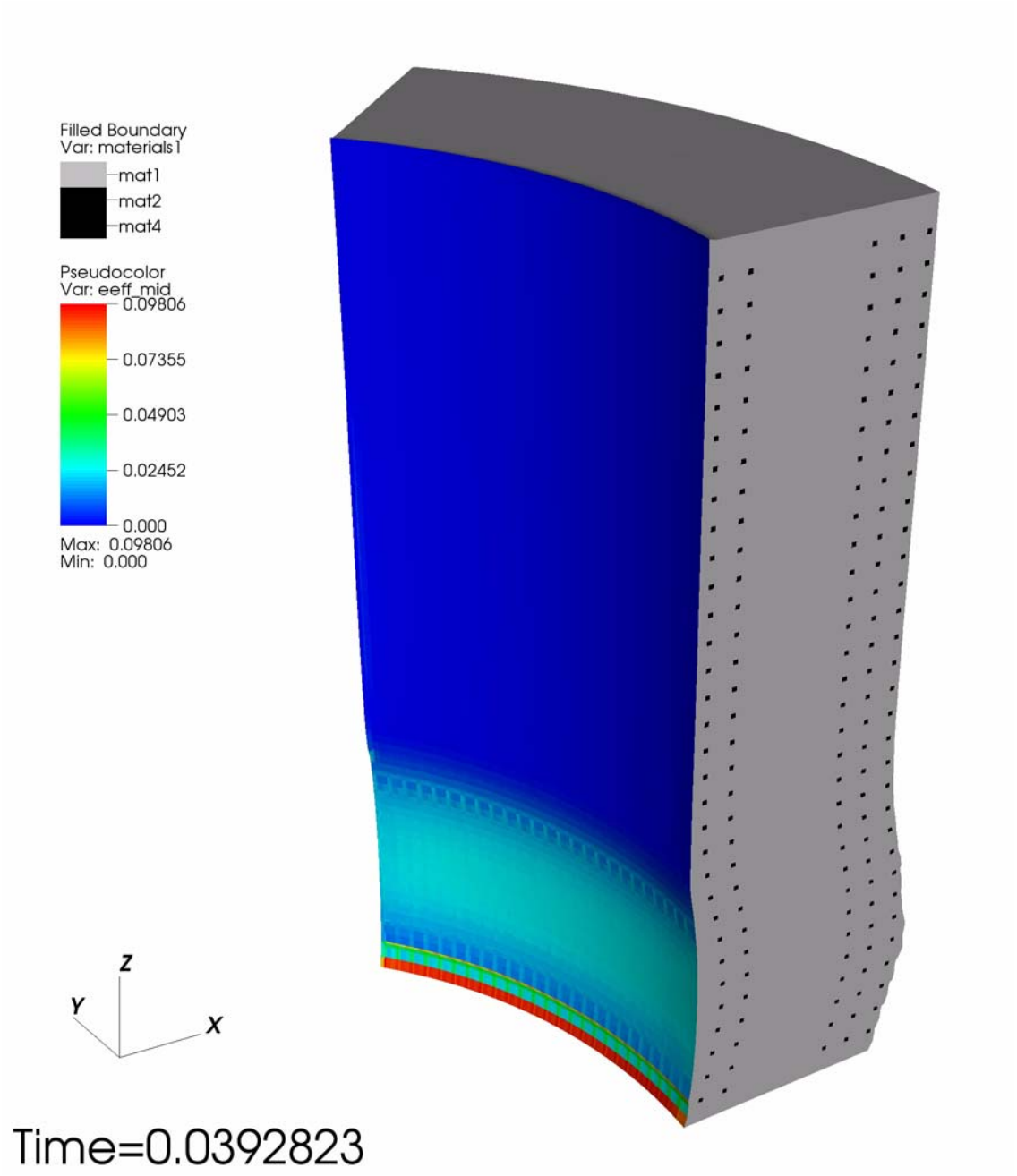

FIGURE 6. Steel liner effective plastic strain pseudocolor plot (taken at the mid-point of the shell element) for the 200 KPa-sec case.

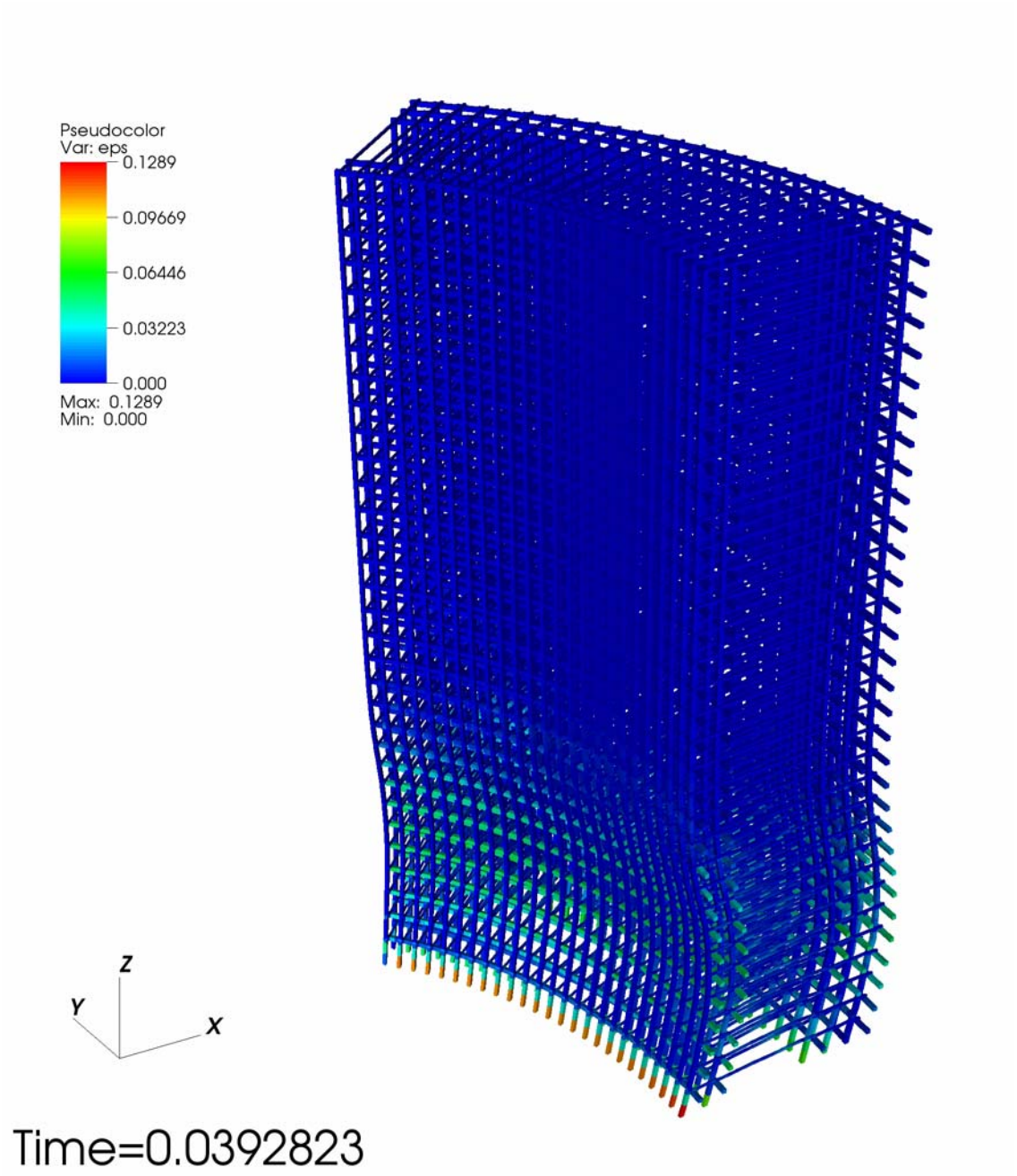

FIGURE 7. Rebar effective plastic strain pseudocolor plot for 200 KPa-sec case.

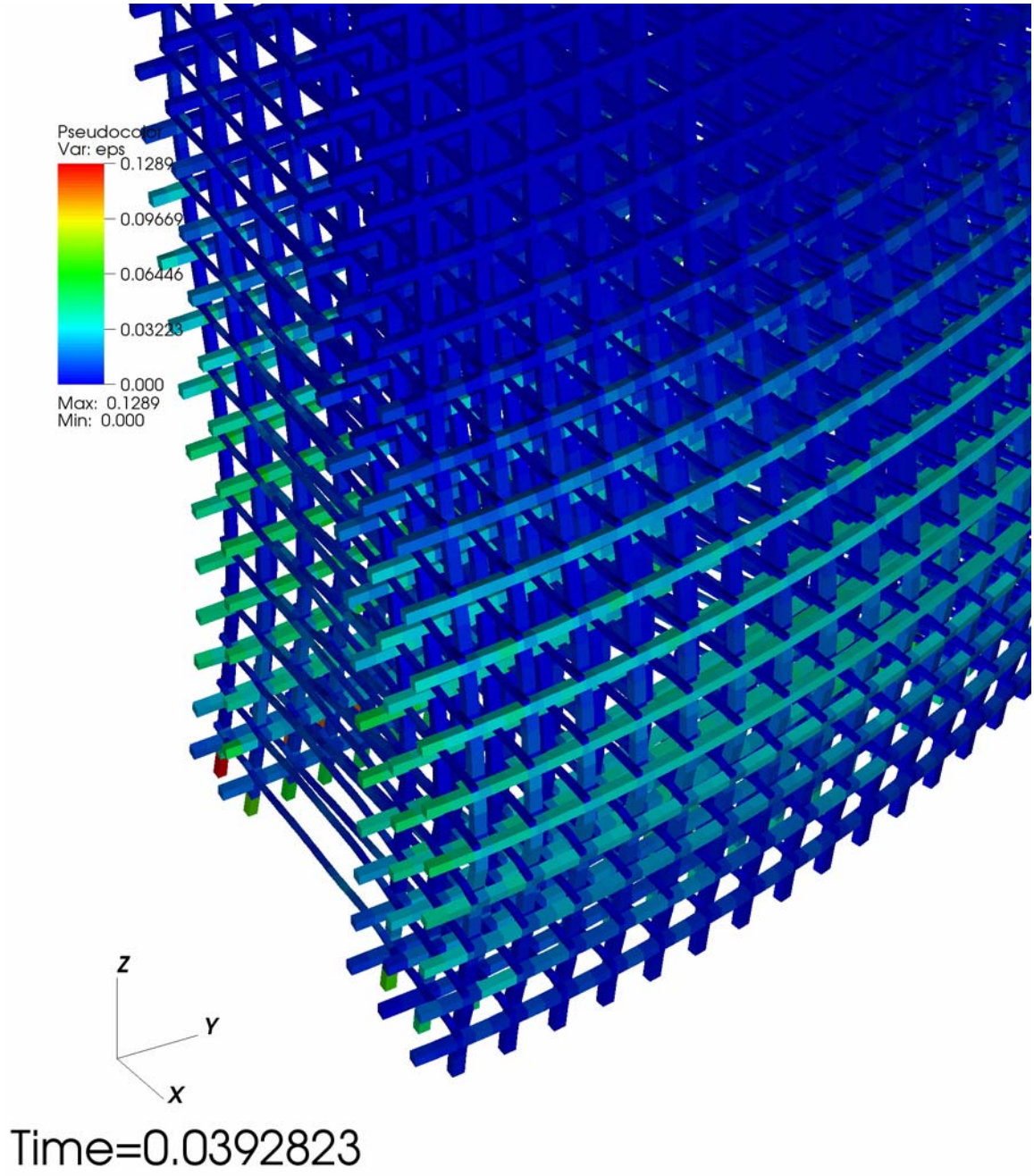

Backside view

FIGURE 8. Blown up view of rebar effective plastic strain at base of model for 200 KPa-sec case.

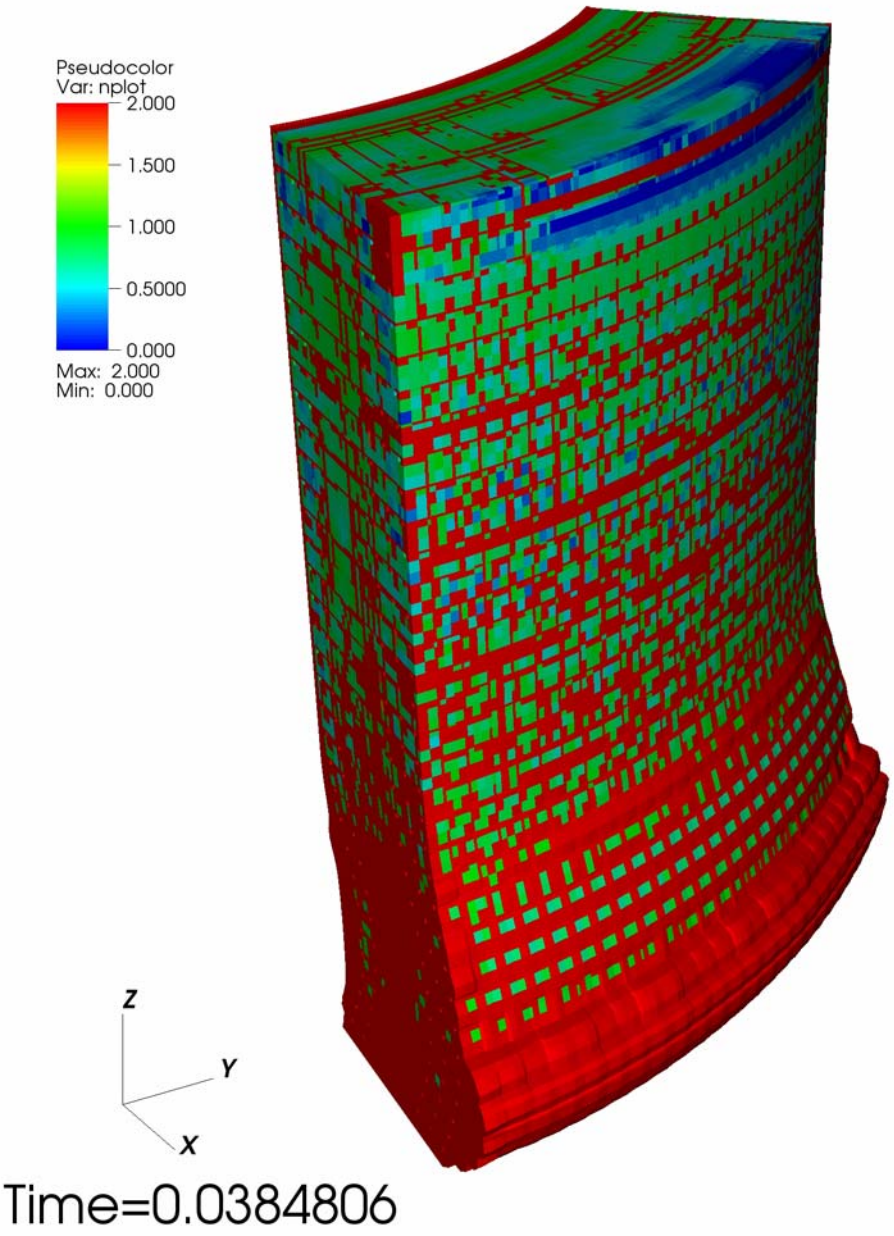

FIGURE 9. Concrete damage pseudocolor plot for 300 KPa-sec case.

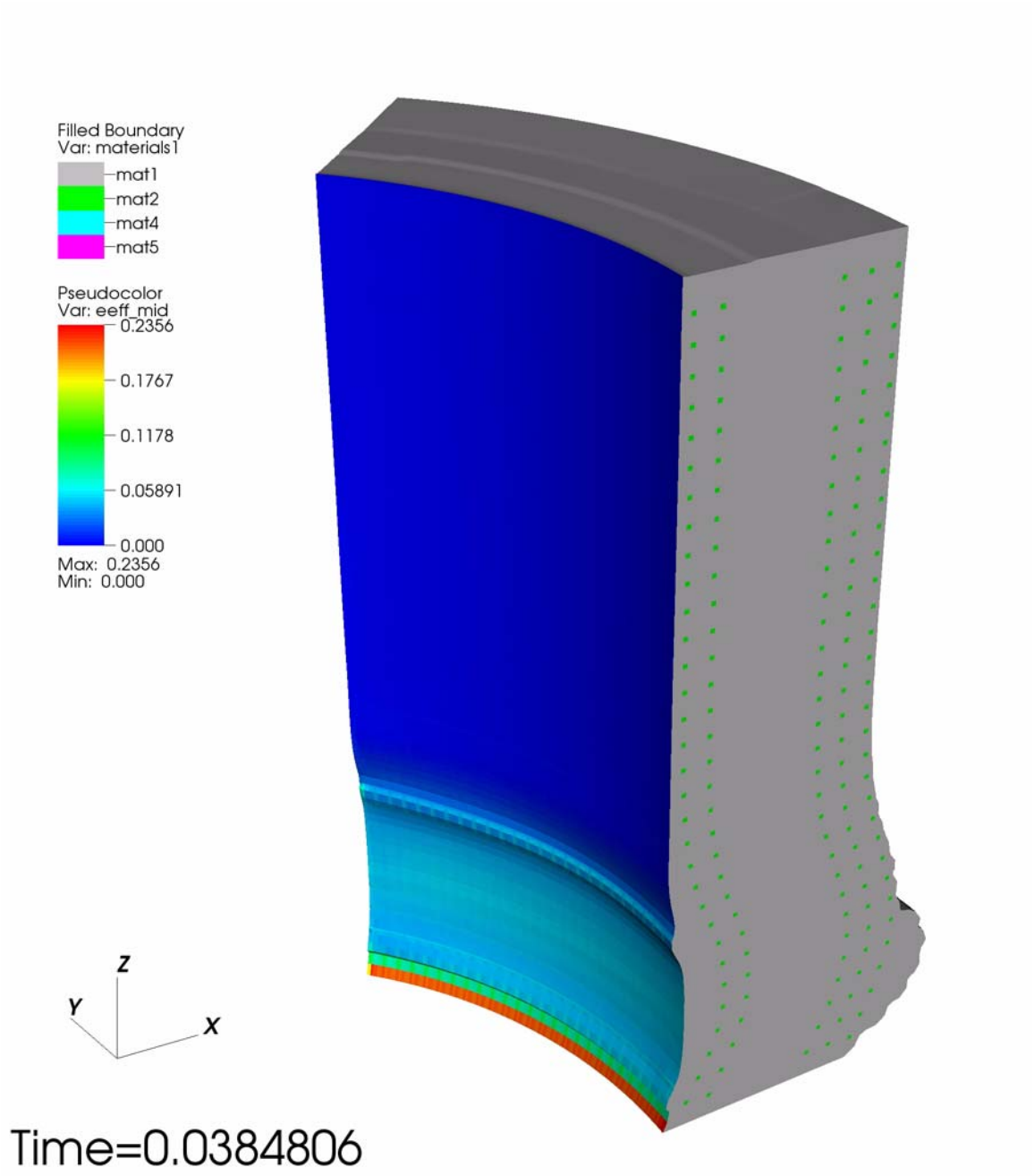

FIGURE 10. Steel liner effective plastic strain pseudocolor plot (taken at the mid-point of the shell element) for the 300 KPa-sec case.

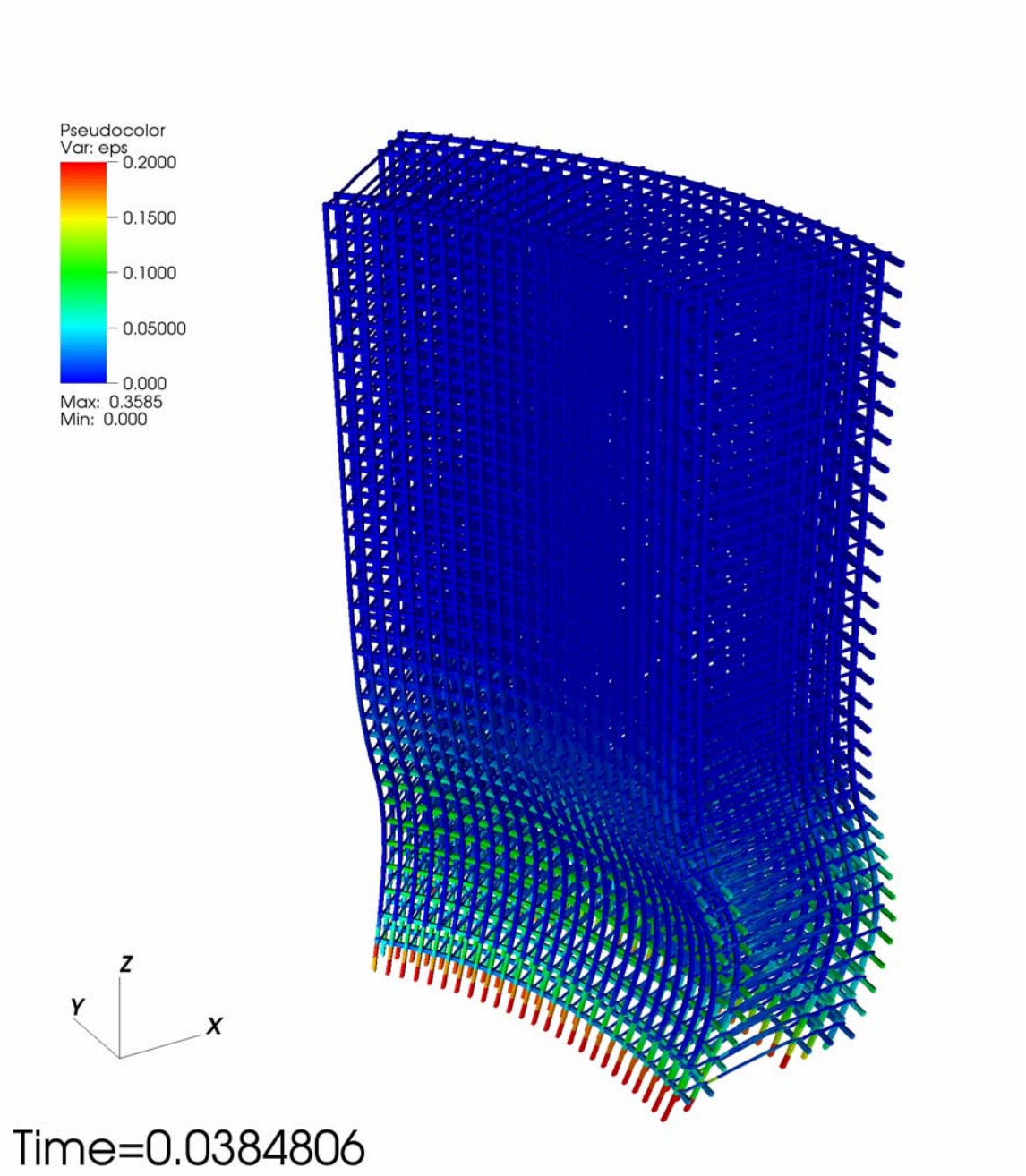

FIGURE 11. Rebar effective plastic strain pseudocolor plot for 300 KPa-sec case.

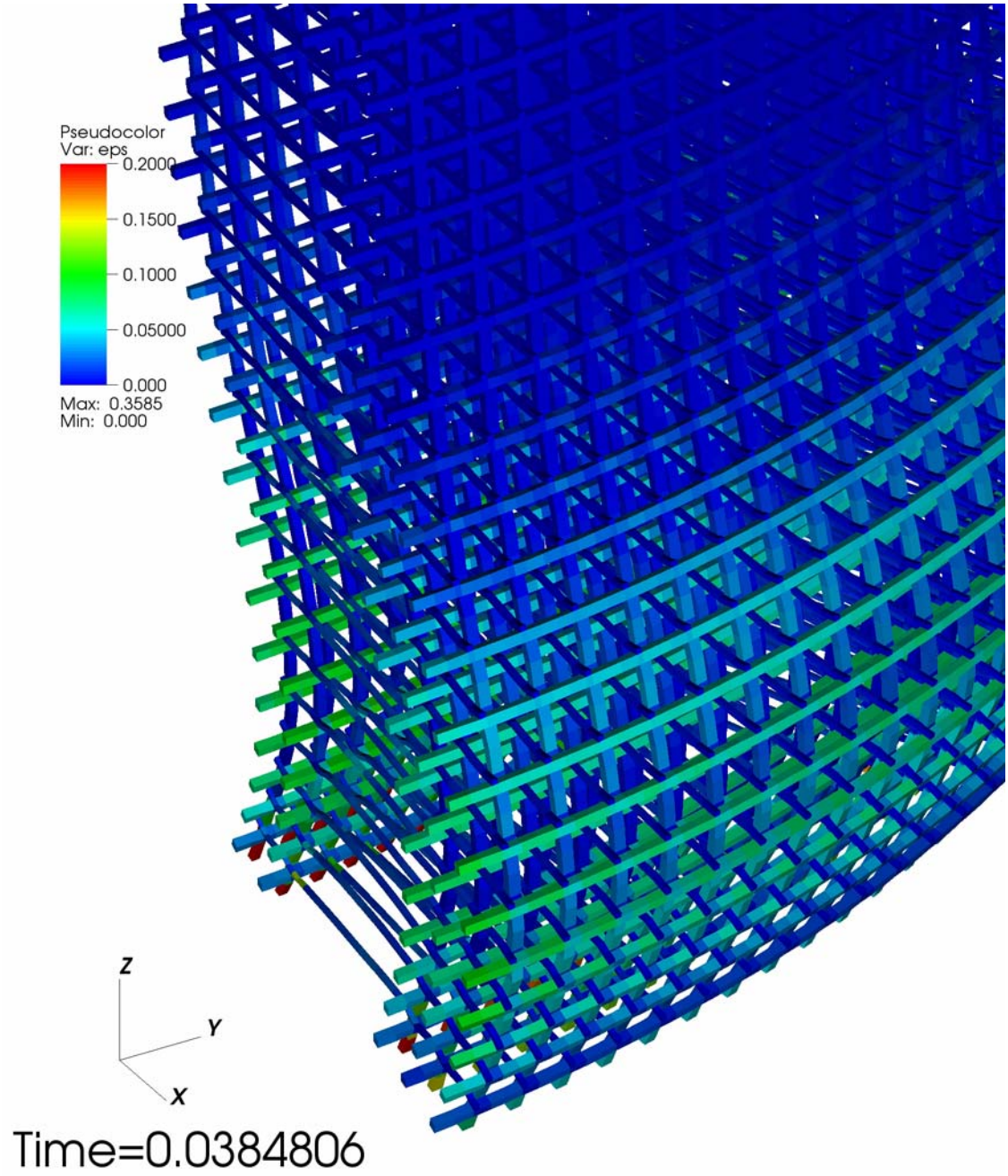

Backside view

FIGURE 12. Blown up view of rebar effective plastic strain at base of model for 300 KPa-sec case.

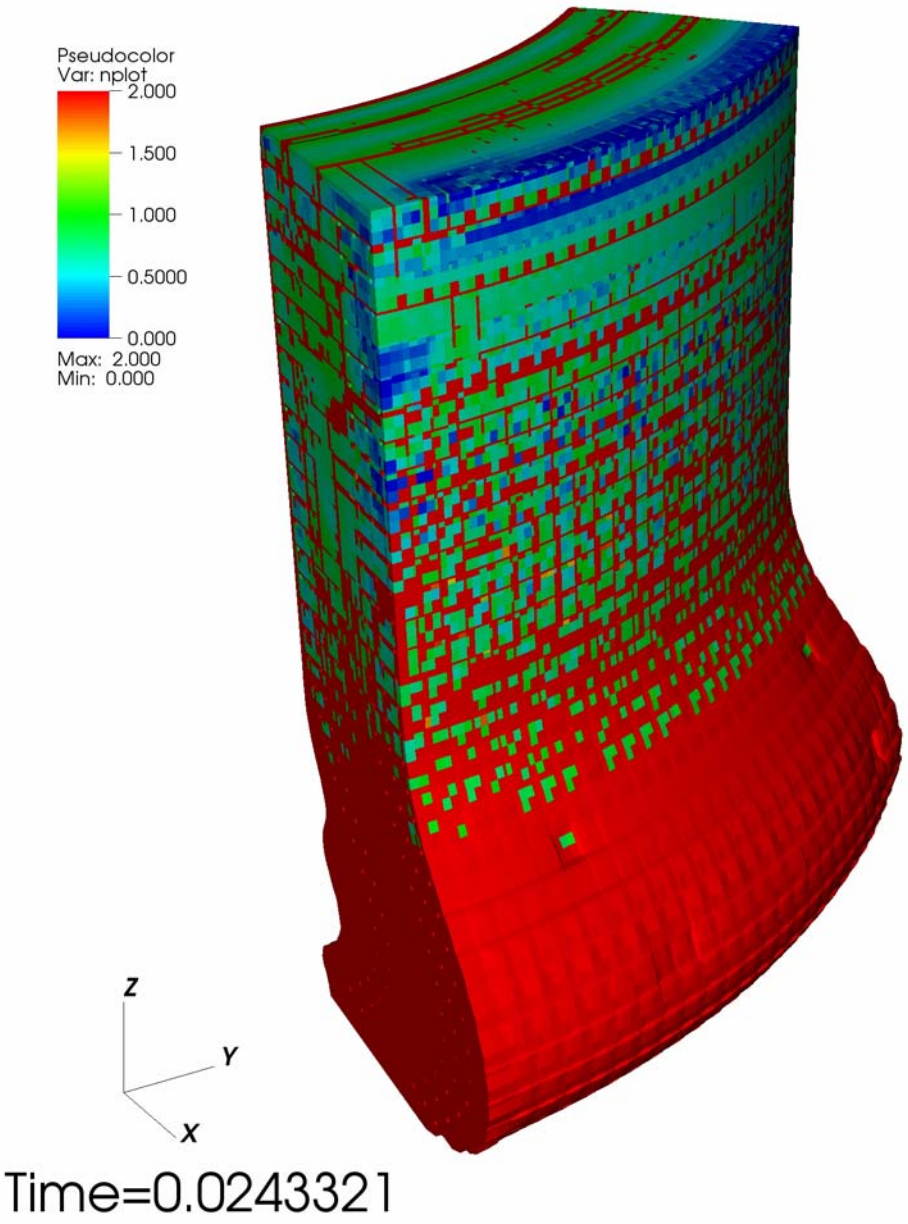

FIGURE 13. Concrete damage pseudocolor plot for 600 KPa-sec case.

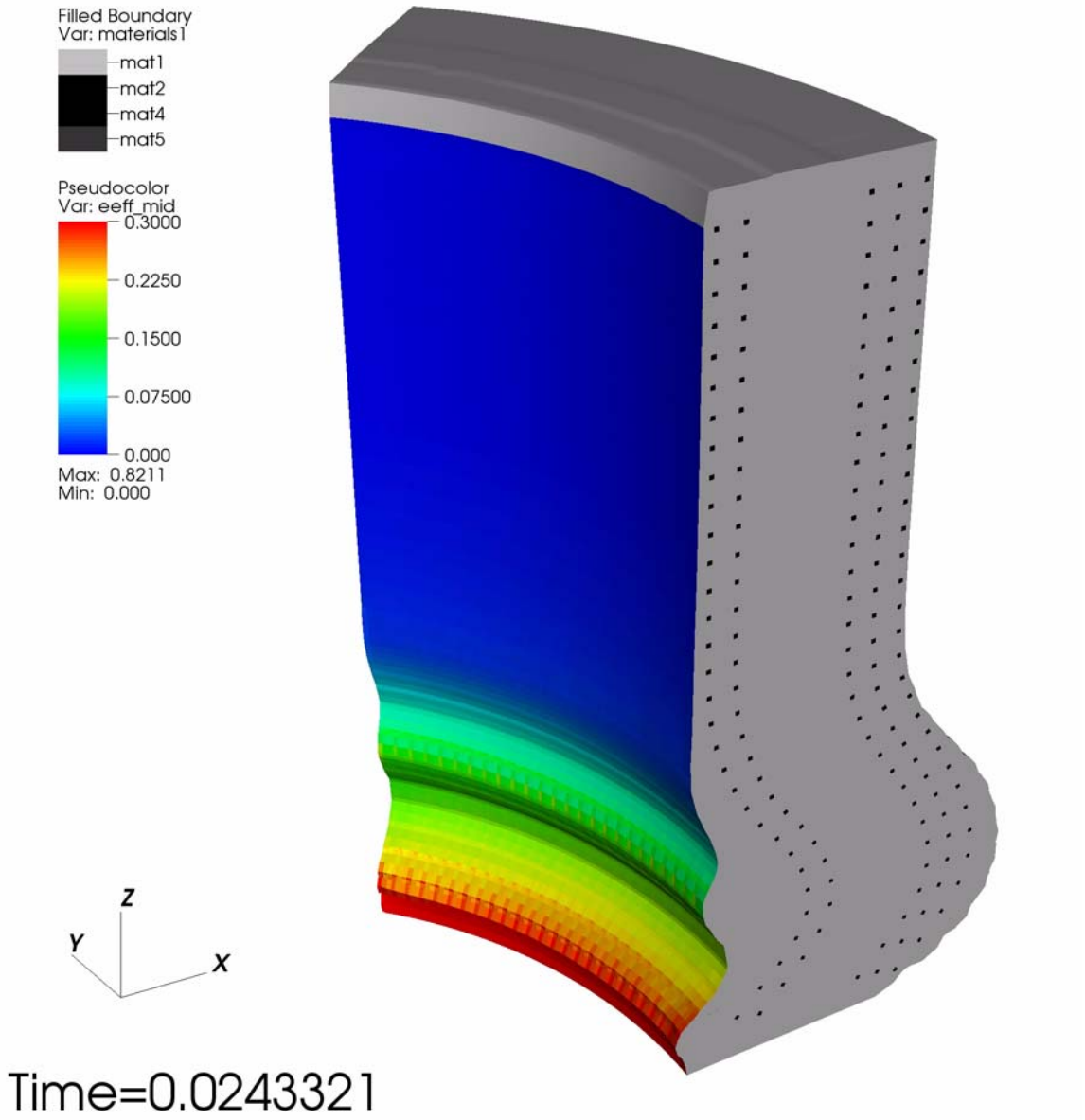

FIGURE 14. Steel liner effective plastic strain pseudocolor plot (taken at the mid-point of the shell element) for the 600 KPa-sec case.

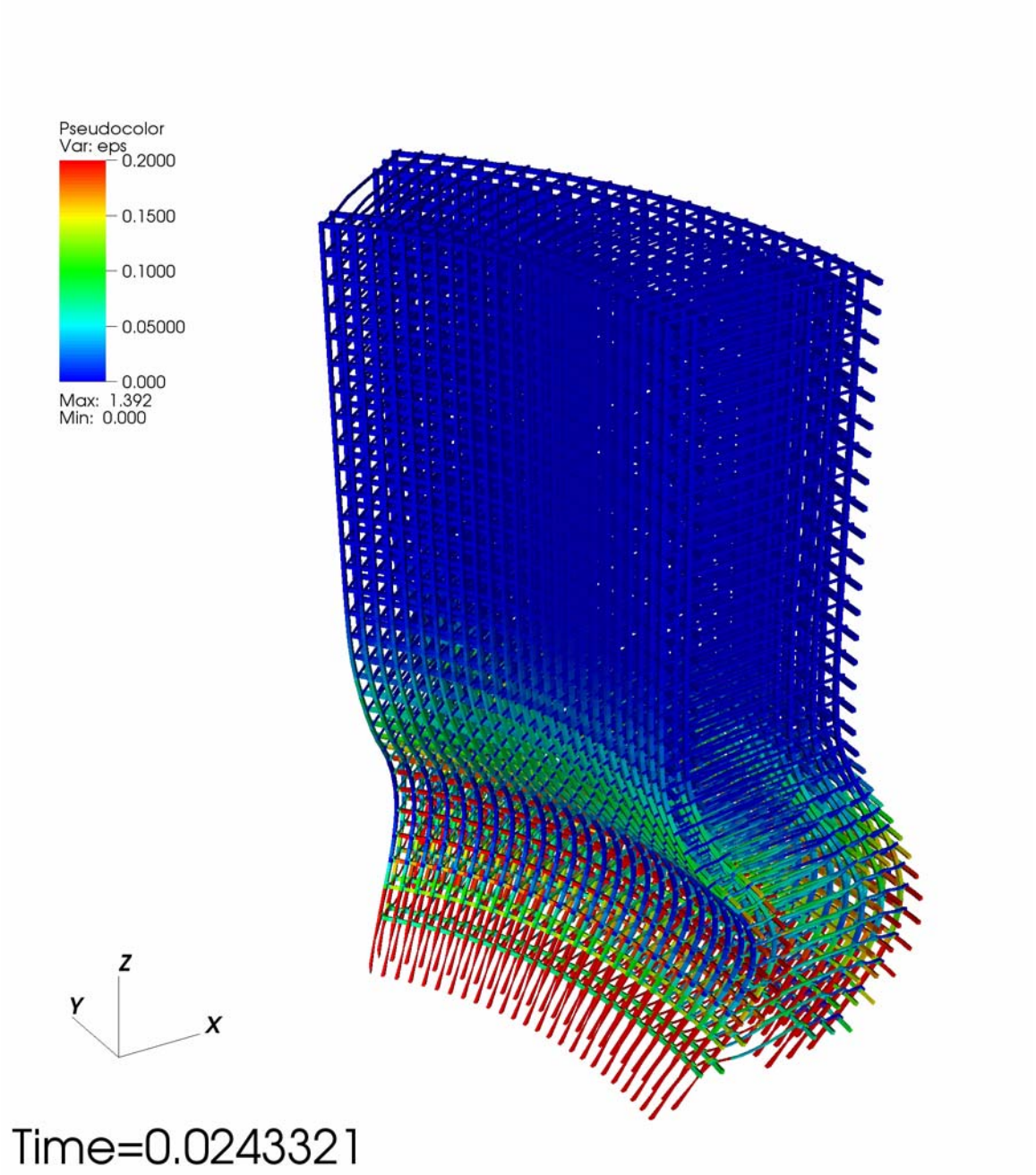

FIGURE 15. Rebar effective plastic strain pseudocolor plot for 600 KPa-sec case.

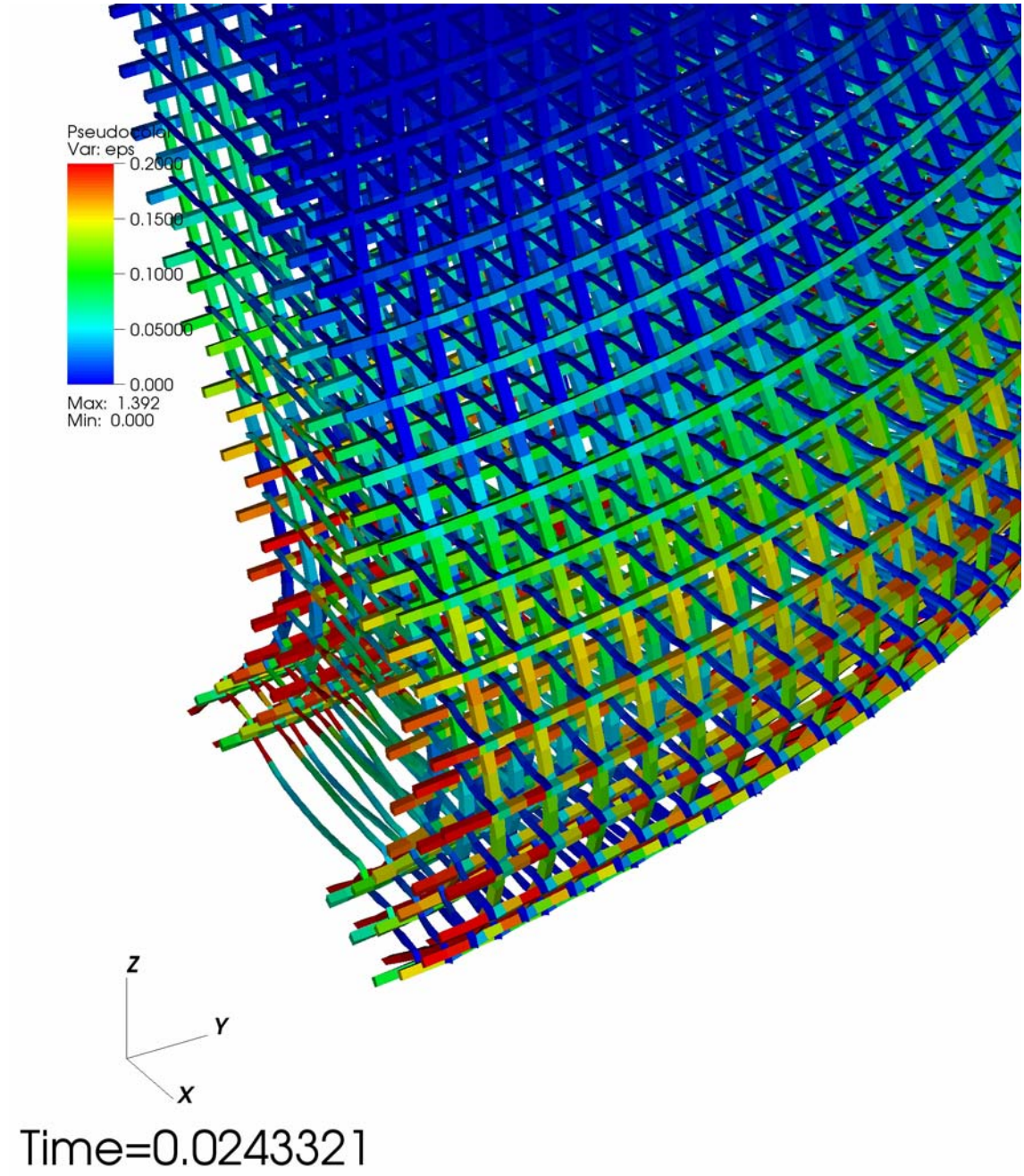

Backside view

FIGURE 16. Blown up view of rebar effective plastic strain at base of model for 600 KPa-sec case.

Appendix

1.0 Background

Concrete is perhaps one of the most widely used construction materials in the world. Engineers use it to build massive concrete dams, concrete waterways, highways, bridges, and even nuclear reactors. The advantages of using concrete is that it can be cast into any desired shape, it is durable, and very economical compared to structural steel. The disadvantages are its low tensile strength, low ductility, and low strength-to-weight ratio. Concrete is a composite material that consists of a coarse granular material, or aggregate, embedded in a hard matrix of material, or cement, which fills the gaps between the aggregates and binds them together. Concrete properties, however, vary widely. The properties depend on the choice of materials used and the proportions for a particular application, as well as differences in fabrication techniques. Table 1 provides a listing of typical engineering properties for structural concrete.

TABLE 1. Typical Engineering Properties of Structural Concrete

Compressive strength	5000 lb/in.^{2}
Tensile strength	400 lb/in.^{2}
Modulus of Elasticity	4 x 10^6 lb/in.^{2}
Poisson's Ratio	0.18
Failure Strain for Unconfined Uniaxial Compression Test	0.002
Failure Strain for Unconfined Uniaxial Tensile Test	0.00012
Coefficient of Thermal Expansion	5.6 x 10^{-6} / ^{o}F
Normal Weight Density	145 lb/ft.^{3}
Lightweight Density	110 lb/ft.^{3}

Properties also depend on the level of concrete confinement, or hydrostatic pressure, the material is being subjected to. In general, concrete is rarely subjected to a single axial stress. The material may experience a combination of stresses all acting simultaneously. The behavior of concrete under these combined stresses are, however, extremely difficult to characterize. In addition to the type of loading, one must also consider the stress history of the material. Failure is determined not only by the ultimate stresses, but also by the rate of loading and the order in which these stresses were applied.

The concrete model described herein accounts for this complex behavior of concrete. It was developed by Javier Malvar, Jim Wesevich, and John Crawford of Karagozian and Case, and Don Simon of Logicon RDA in support of the Defense Threat Reduction Agency's programs. The model is an enhanced version of the Concrete/Geological Material Model 16 in the Lagrangian finite element code DYNA3D. The modifications that were made to the original model ensured that the material response followed experimental observations for standard uniaxial, biaxial, and triaxial tests for both tension and compression type loading. A disadvantage of using this material model, however, is the overwhelming amount of input that is required from the user. Therefore, the goal of this report is to provide future users with the tools necessary for successfully using this model.

1.1 Terminology

Before discussing the details of this model, it is instructive to provide an overview of some of the key terminology and nomenclature that will be used extensively later on in this description.

1.1.1 Volumetric and Deviatoric Stresses and Strains

As you may recall, stress can be broken up into its volumetric and deviatoric parts as follows,

$$\sigma = \sigma_M + s \tag{EQ 1}$$

In indicial form,

$$\sigma_{M_{ij}} = \frac{1}{3}\sigma_{kk}\delta_{ij} \qquad \text{or} \qquad \sigma_{M_{ij}} = p\delta_{ij} \tag{EQ 2}$$

where

$$p = \frac{1}{3}\sigma_{kk} \qquad \text{or} \qquad p = \frac{1}{3}(\sigma_{11} + \sigma_{22} + \sigma_{33}) \tag{EQ 3}$$

and

$$s_{ij} = \sigma_{ij} - \frac{1}{3}\sigma_{kk}\delta_{ij} \tag{EQ 4}$$

However, in DYNA3D, pressure is defined as the negative of the one defined above,

$$p = -\frac{1}{3}(\sigma_{11} + \sigma_{22} + \sigma_{33}) \tag{EQ 5}$$

so that pressure is positive in compression.

In addition, for a principal coordinate system that coincides with the directions of the principal stresses, all the σ_{ij}, with $i \neq j$, terms vanish so that

$$p = \frac{1}{3}(\sigma_1 + \sigma_2 + \sigma_3) \tag{EQ 6}$$

and

$$s_1 = max\{\sigma_1 - p, \sigma_2 - p, \sigma_3 - p\} \tag{EQ 7}$$

Finally, volumetric and deviatoric strains are commonly written as,

$$\varepsilon_v = \varepsilon_1 + \varepsilon_2 + \varepsilon_3$$
$$\varepsilon_q = \frac{2}{3}(\varepsilon_1 - \varepsilon_3) \quad \text{(EQ 8)}$$

1.1.2 Stress Invariants

Scalar quantities may also be constructed out of the tensor σ_{ij}, that is,

$$P_1 = \sigma_{ii}$$
$$P_2 = \sigma_{ij}\sigma_{ij} \quad \text{(EQ 9)}$$
$$P_3 = \sigma_{ij}\sigma_{jk}\sigma_{ki}$$

These scalar quantities constructed from a tensor are independent of any particular coordinate system and are therefore known as invariants. In the principal coordinate frame, these quantities are usually written as,

$$P_1 = \sigma_1 + \sigma_2 + \sigma_3$$
$$P_2 = \sigma_1^2 + \sigma_2^2 + \sigma_3^2 \quad \text{(EQ 10)}$$
$$P_3 = \sigma_1^3 + \sigma_2^3 + \sigma_3^3$$

In this particular model description, however, the stress invariants are defined as follows,

$$I_1 = 3p = (\sigma_1 + \sigma_2 + \sigma_3)$$
$$J_2 = \frac{1}{2}(s_1^2 + s_2^2 + s_3^2) \qquad \text{or}$$
$$\sqrt{J_2} = \frac{\sqrt{(\sigma_1 - \sigma_2)^2 + (\sigma_1 - \sigma_3)^2 + (\sigma_2 - \sigma_3)^2}}{\sqrt{6}} \quad \text{(EQ 11)}$$
$$J_3 = s_1 s_2 s_3$$

1.1.3 Triaxial Compression and Extension

The triaxial compression test provides the means for defining the effect of confinement on the strength of the concrete. When a lateral confining pressure is applied, the increase in compressive strength can be very large. In addition, the application of a lateral confining pressure leads to a large increase in the compressive strain at failure. The effect of a confining pressure on strength is, however, more beneficial for weak than for strong con-

cretes. In the case of tension plus biaxial compression, the tensile strength is reduced by the application of lateral compressive stresses.

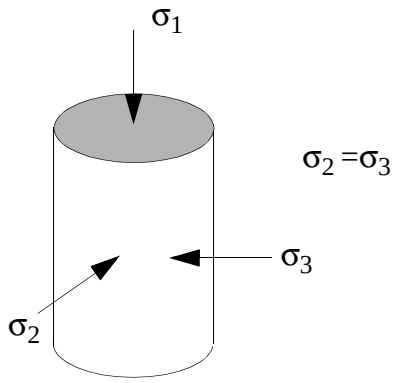

FIGURE 1. Description of triaxial test

A typical triaxial compression test is defined as follows:

1. at the beginning of the test, $\sigma_1 = \sigma_2 = p$.
2. during test, σ_1 increased until failure.
3. At failure, the concrete strength is defined as $\Delta\sigma_c = |\sigma_1 - \sigma_2|$.

A typical triaxial extension test is defined as follows:

1. at the beginning of the test, $\sigma_1 = \sigma_2 = p$.
2. during test, σ_1 increased until failure.
3. At failure, the concrete strength is defined as $\Delta\sigma_t = |\sigma_1 - \sigma_2|$.

A comparison of the concrete strengths may be computed as

$$\psi = \frac{\Delta\sigma_t}{\Delta\sigma_c} \qquad \text{(EQ 12)}$$

The value, ψ, usually varies from $0.5 \le \psi \le 1.0$, depending on the amount of confining pressure the material is subjected to.

The $\Delta\sigma$ value defined above will be used throughout the material description as a way of referring to the shear strength of concrete. The $\Delta\sigma$ can also be related to the second invariant of the deviatoric stress by

$$\Delta\sigma = \sqrt{3J_2} \qquad \text{(EQ 13)}$$

2.0 Nonlinear Concrete Model Description

The Karagozian & Case concrete model decouples the volumetric and deviatoric responses. The model also uses an Equation of State (EOS). The Equation of State prescribes a user-defined set of pressures, unloading bulk moduli, and volumetric strains. Once the pressure has been determined from the EOS, a movable surface, or failure surface, limits the second invariant of the deviatoric stress tensor (i.e. $\Delta\sigma$). In addition, the model is strain rate dependent, which is extremely important for accurately simulating blast effects.

2.1 Failure Surfaces

The model uses three independent fixed surfaces to define the plastic behavior of concrete. The surfaces, which define three important regions of concrete behavior, can be seen easily if one plots the stress-strain response from an unconfined uniaxial compression test (see Figure 2). The material response is considered linear up until point 1, or first yield. After yielding, a hardening plasticity response occurs until point 2, or maximum strength, is reached. After reaching a maximum strength, softening occurs until a residual strength, which is based on the amount of confinement, is obtained. The three surfaces are defined by the following equations:

$$\Delta\sigma_y = a_{oy} + \frac{p}{a_{1y} + a_{2y}p} \qquad \text{(yield failure surface)} \qquad \text{(EQ 14)}$$

$$\Delta\sigma_m = a_o + \frac{p}{a_1 + a_2 p} \qquad \text{(maximum failure surface)} \qquad \text{(EQ 15)}$$

$$\Delta\sigma_r = \frac{p}{a_{1f} + a_{2f}p} \qquad \text{(residual failure surface)} \qquad \text{(EQ 16)}$$

where a_{oy}, a_{1y}, a_{2y}, a_o, a_1, a_2, a_{1f}, and a_{2f} are all user-defined parameters which change the shape of the failure surface.

The current failure surface is calculated from the three fixed surfaces using a simple linear interpolation technique:

1. if the current state lies between the yield surface and the maximum surface, the failure surface is calculated using

$$\Delta\sigma_f = \eta(\Delta\sigma_m - \Delta\sigma_y) + \Delta\sigma_y \qquad \text{(EQ 17)}$$

2. if, on the other hand, the current state is located between the maximum surface and the residual surface, the failure surface is defined by

$$\Delta\sigma_f = \eta(\Delta\sigma_m - \Delta\sigma_r) + \Delta\sigma_r \qquad \text{(EQ 18)}$$

where η varies between 0 and 1, and depends on the accumulated effective plastic strain parameter λ. The current value of λ - calculated using an equation that will be discussed later - is compared to a set of 13 user-defined (η, λ) pairs, which are usually determined from experimental data.The η value is 0 when $\lambda = 0$, 1 at some value $\lambda = \lambda_m$, and again 0 at some larger value of λ. Therefore, if $\lambda \leq \lambda_m$, the current failure surface is calculated using EQ. 17, and if $\lambda \geq \lambda_m$, the current failure surface is calculated using EQ. 18. In essence, the (η, λ) values define where the current failure surface is in relation to the three fixed surfaces for different values of plastic strain.

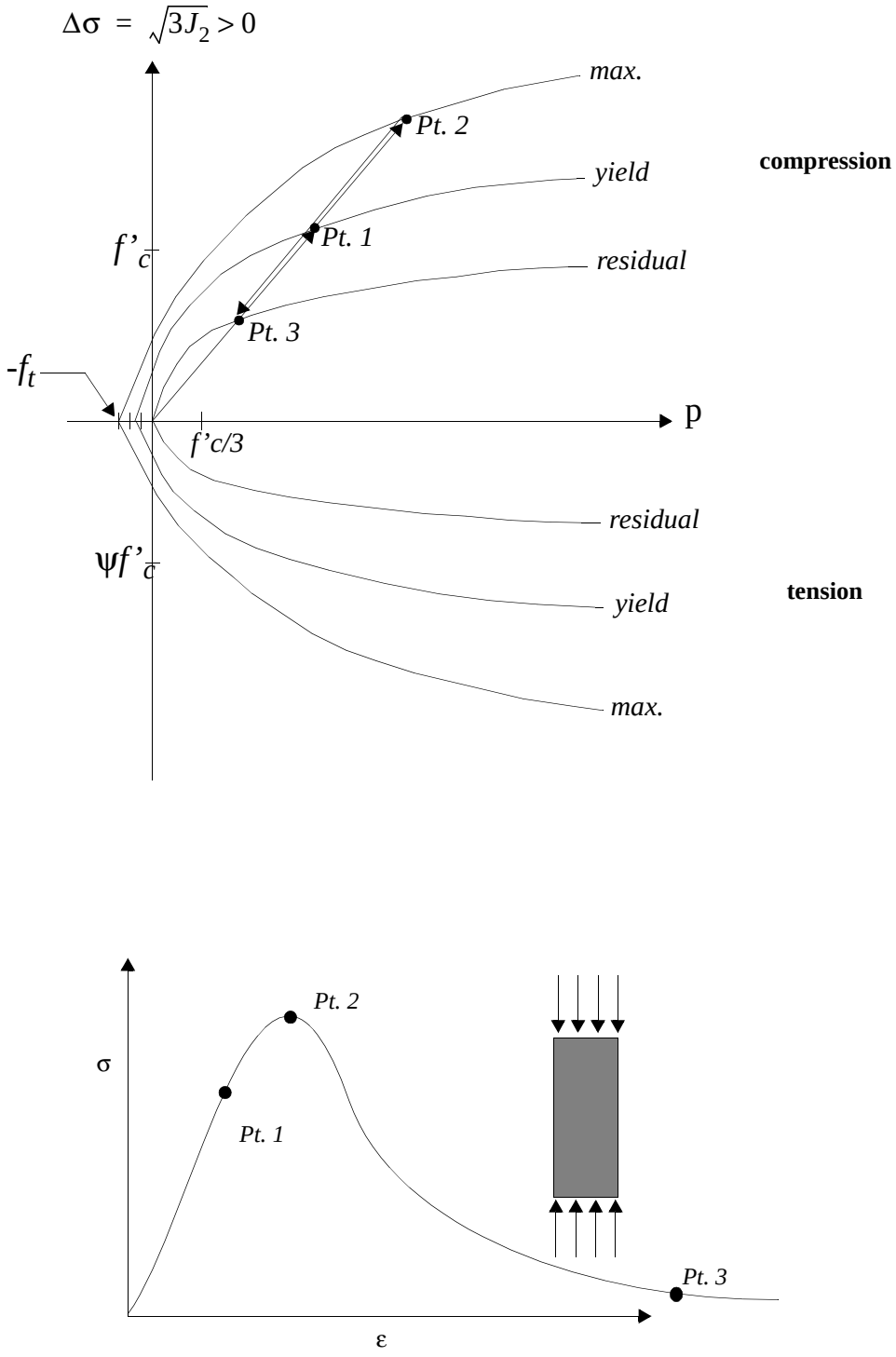

FIGURE 2. Model failure surfaces and uniaxial stress-strain response

2.2 Pressure Cutoff

The pressure cutoff was modified from the original DYNA3D material model 16 to prevent the pressure from being lower than the maximum tensile strength f_t, instead of $f_t/3$. This allows for correct values of $\Delta\sigma$ for both the biaxial and triaxial tensile tests (see Figure 3). For example, the uniaxial, biaxial, and triaxial $\Delta\sigma$ values are calculated as follows:

1. *Uniaxial:* $(\sigma_1 = f_t, \sigma_2 = 0, \sigma_3 = 0)$

$$\sqrt{J_2} = \frac{\sqrt{(\sigma_1-\sigma_2)^2 + (\sigma_1-\sigma_3)^2 + (\sigma_2-\sigma_3)^2}}{\sqrt{6}} = \frac{f_t}{\sqrt{3}}$$

$$\Delta\sigma = f_t$$

$$p = -\frac{f_t}{3}$$

2. *Biaxial:* $(\sigma_1 = f_t, \sigma_2 = f_t, \sigma_3 = 0)$

$$\sqrt{J_2} = \frac{\sqrt{(\sigma_1-\sigma_2)^2 + (\sigma_1-\sigma_3)^2 + (\sigma_2-\sigma_3)^2}}{\sqrt{6}} = \frac{f_t}{\sqrt{3}}$$

$$\Delta\sigma = f_t$$

$$p = -\frac{2f_t}{3}$$

3. *Triaxial:* $(\sigma_1 = f_t, \sigma_2 = f_t, \sigma_3 = f_t)$

$$\sqrt{J_2} = \frac{\sqrt{(\sigma_1-\sigma_2)^2 + (\sigma_1-\sigma_3)^2 + (\sigma_2-\sigma_3)^2}}{\sqrt{6}} = 0$$

$$\Delta\sigma = 0$$

$$p = -f_t$$

When the material has failed in the negative pressure range, the previously defined parameter η is used to increase the pressure cutoff from $-f_t$ to zero. The pressure cutoff, p_c, is calculated from the following rule (see Figure 3):

1. p_c is equal to $-f_t$ if the maximum failure surface has not yet been reached.

2. p_c is equal to $-\eta f_t$ if the maximum failure surface has already been reached.

This pressure cutoff is needed because the EOS may calculate very large negative pressures for large volumetric extensions beyond cracking, which is, of course, physically unrealistic.

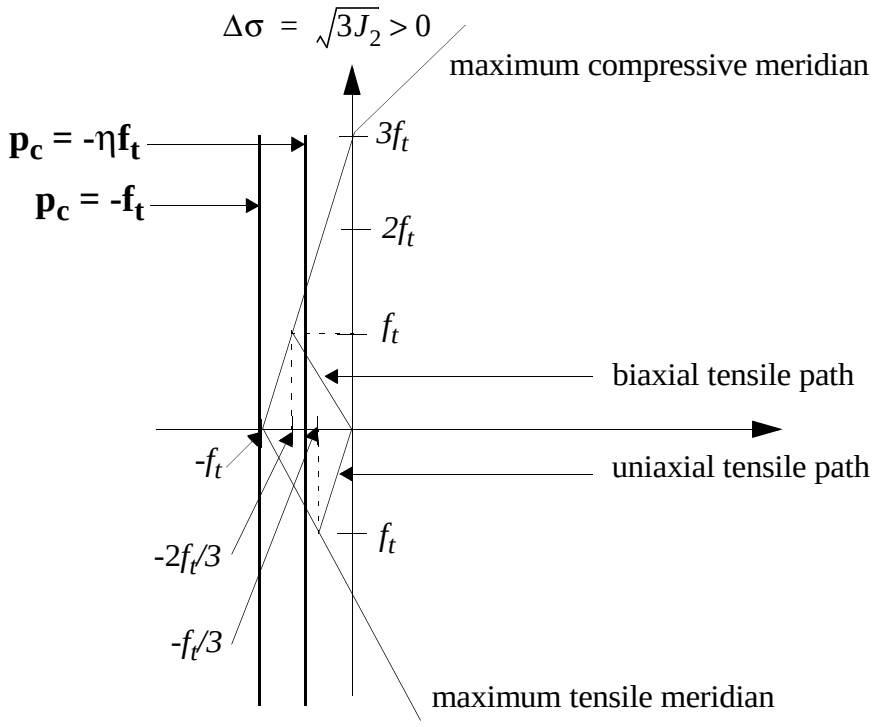

FIGURE 3. Description of pressure cutoff and tensile paths

2.3 Damage Evolution

As you may recall, the current failure surface is interpolated between either the yield and maximum surface or the maximum and residual surface using a set of user-defined (η, λ) pairs. The current value of the damage parameter λ is defined using the following relationships:

$$\lambda = \int_0^{\bar{\varepsilon}^p} \frac{\overline{d\varepsilon^p}}{r_f\left(1 + \frac{p}{r_f f_t}\right)^{b_1}} \qquad \text{when} \qquad p \geq 0 \tag{EQ 19}$$

$$\lambda = \int_0^{\bar{\varepsilon}^p} \frac{\overline{d\varepsilon^p}}{r_f\left(1 + \frac{p}{r_f f_t}\right)^{b_2}} \qquad \text{when} \qquad p < 0 \tag{EQ 20}$$

where the effective plastic strain increment is given by:

$$\overline{d\varepsilon^p} = \sqrt{\left(\frac{2}{3}\right) d\varepsilon_{ij}^p d\varepsilon_{ij}^p} \tag{EQ 21}$$

It is instructive to mention that this effective plastic strain increment is the one commonly used for a von Mises isotropic hardening model for metals. In a more general case, the effective plastic strain increment is defined as:

$$\overline{d\varepsilon^p} = \sqrt{\left(\frac{2}{3}\right) de_{ij}^p de_{ij}^p} \qquad \text{or in the longer format}$$

$$\left(\overline{d\varepsilon^p} = \left\{\frac{2}{9}\left[\left(d\varepsilon_{11}^p - d\varepsilon_{22}^p\right)^2 + \left(d\varepsilon_{22}^p - d\varepsilon_{33}^p\right)^2 + \left(d\varepsilon_{33}^p - d\varepsilon_{11}^p\right)^2\right] + \frac{4}{3}\left[\left(d\varepsilon_{23}^p\right)^2 + \left(d\varepsilon_{31}^p\right)^2 + \left(d\varepsilon_{12}^p\right)^2\right]\right\}^{\frac{1}{2}}\right) \tag{EQ 22}$$

where e_{ij} is the deviatoric part of strain and can be written,

$$e_{ij}^p = \varepsilon_{ij}^p - \frac{1}{3}\delta_{ij}\varepsilon_{kk}^p \tag{EQ 23}$$

The reasoning behind writing the effective plastic strain increment as in EQ. 21, is that when modeling metals, it is postulated that the plastic deformation occurs under constant volume (i.e. $\varepsilon_{kk}^p = 0$). This assumption forces $e_{ij}^p = \varepsilon_{ij}^p$. The drawback of using a deviatoric damage criterion for concrete, is that the material cannot accumulate damage under a pure volumetric extension, or triaxial tensile test, because the second deviatoric stress invariant remains zero. Therefore, a volumetric damage increment was added to the deviatoric damage whenever the stress path was “close” to the triaxial tensile test path. The closeness to this path is calculated from the ratio $\left|(\sqrt{3J_2})/p\right|$, which is 1.5 for the biaxial tensile test, as you may recall from the pressure cutoff examples. The volumetric damage increment is limited by a closeness parameter f_d given by

$$f_d = \begin{cases} 1 - \dfrac{\left|(\sqrt{3J_2})/p\right|}{0.1} & , 0 \le \left|(\sqrt{3J_2})/p\right| < 0.1 \\ 0 & , \left|(\sqrt{3J_2})/p\right| \ge 0.1 \end{cases} \quad \text{(EQ 24)}$$

Then the modified effective plastic strain damage parameter is incremented by

$$\Delta\lambda = b_3 f_d k_d (\varepsilon_v - \varepsilon_{v,\,yield}) \quad \text{(EQ 25)}$$

where b_3 is a user-defined parameter that prescribes the rate of damage primarily in the triaxial tensile regime, k_d is an internal scalar multiplier, and ε_v and $\varepsilon_{v,\,yield}$ are the volumetric strain and volumetric strain at yield.

The user-defined parameters b_1 and b_2, located in EQ. 19 and EQ. 20, also change the rate at which damage occurs, and the r_f value is a dynamic increase factor that accounts for strain rate effects. It is important to note that the DYNA3D manual states EQ. 19 and EQ. 20 as follows:

$$d\lambda = \frac{\overline{d\varepsilon^p}}{\left[1 + \left(\frac{s}{100}\right)(r_f - 1)\right]\left(1 + \frac{p}{r_f f_t}\right)^{b_1}} \quad \text{when} \quad p \ge 0 \quad \text{(EQ 26)}$$

$$d\lambda = \frac{\overline{d\varepsilon^p}}{\left[1 + \left(\frac{s}{100}\right)(r_f - 1)\right]\left(1 + \frac{p}{r_f f_t}\right)^{b_2}} \quad \text{when} \quad p < 0 \quad \text{(EQ 27)}$$

If the user defines s = 0, the strain-rate effects have been toggled off, and if s=100, the strain-rate effects are included.

In addition, the values b_2 and b_3, which govern the softening part of a tensile stress-strain response, are mesh-size dependent. For example, this means that the softening response for a 6 x 6 x 6 in. cube element will likely be different for a 1 x 1 x 1 in. cube element, if the same values of b_2 and b_3 are used to define both element sizes. Therefore, different material definitions should be used for different regions of the finite element model. It is highly recommended that the user perform a series of single element tensile tests to view whether the material model is indeed yielding the desired softening response. If the analysis does not give a realistic stress-strain curve, the b_2 and b_3 parameters should be modified and the tensile test restarted. This iterative procedure should be continued until the

desired result is achieved. Figure 4 shows the variation that can occur for WSMR-5 3/4 concrete.

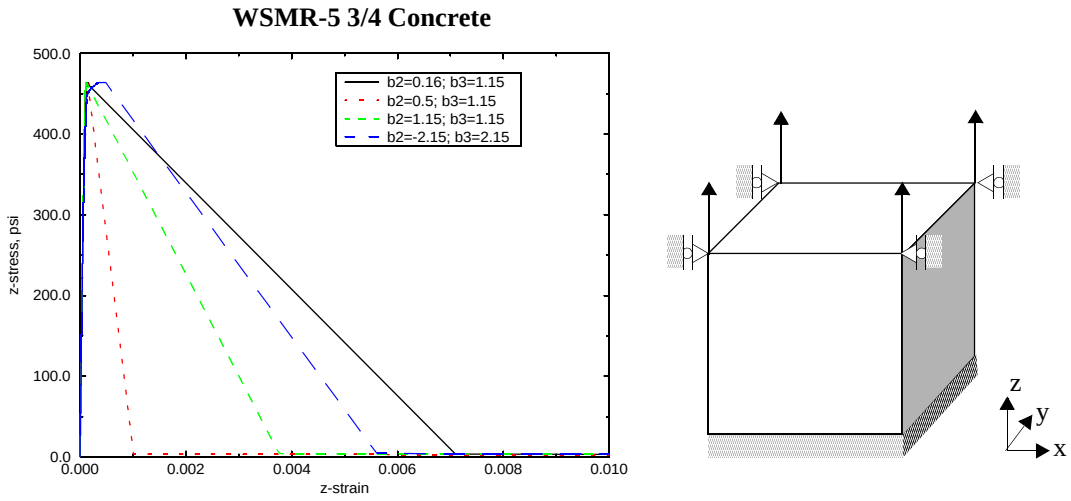

FIGURE 4. Effects of parameters b_2 and b_3 on softening for a single element tensile test.

The user may also track the failure surface evolution by specifying a value of 2 for the emr output on card 4 of the DYNA3D material deck. This parameter tells the subroutine to calculate a "damage" parameter δ, which is calculated in the following manner:

$$\delta = \frac{2\lambda}{\lambda + \lambda_m} \qquad \text{(EQ 28)}$$

This parameter will be a value of 0 until the initial yield surface has been reached, a value of 1 when the failure surface reaches the maximum surface, and a value of 2 at the residual surface.

In addition, an element deletion criteria was added recently. During extreme loading conditions, some elements, after failing in tension, would stretch or deform continuously without any limits. As a result, the time step would decrease until it was no longer feasible to run the simulation. This can be a problem when the user wants to run the simulation out to a far enough time to see the global response of the structure being analyzed. Therefore, the element deletion criterion that seemed to give the best results for this type of situation, was one that was based on a tensile volumetric strain. To use this feature, the user places a volumetric strain value in row 4 of card 4 in the DYNA3D material deck. Once this volumetric strain has been reached, the element is deleted from the simulation. It is recommended that a relatively high value be used, however, otherwise the element may be deleted too soon. Furthermore, if the element being deleted is subjected to a pressure loading at the time of deletion, that pressure loading will not transfer to the surrounding elements.

2.4 Description of Third Invariant

As you may recall, in a three-dimensional principal stress space, the yield surface may be visualized as a prism with the axis along the space diagonal $\sigma_1 = \sigma_2 = \sigma_3$, which is the ray OC shown in Figure 5.

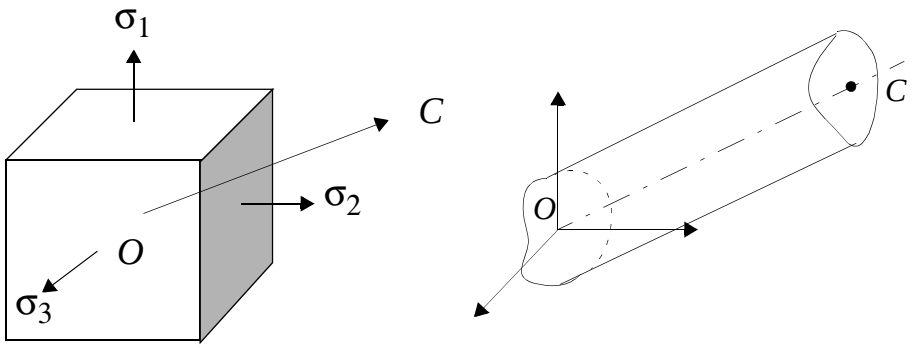

FIGURE 5. Three-dimensional state of stress and space diagonal

Since the stress state may be resolved into a volumetric component and a stress deviator component, the cross section of the prism represents the deviatoric plane. The cross section of the prism may be plotted on any plane perpendicular to the space diagonal. The deviatoric planes have the following equation:

$$\sigma_1 + \sigma_2 + \sigma_3 = \text{constant} \qquad \text{(EQ 29)}$$

where the π-plane is the deviatoric plane that passes through the origin.

As you know, the yield condition attributed to R. von Mises is represented by a circle on the π-plane (see Figure 6). The circle is the intersection of a sphere of radius r

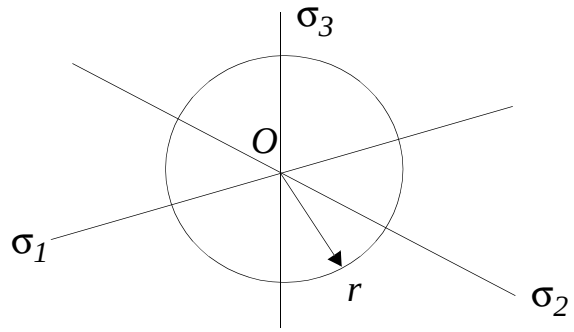

FIGURE 6. Von Mises yield surface (plan view of π-plane).

$$\sigma_1^2 + \sigma_2^2 + \sigma_3^2 = r^2 \quad \text{(EQ 30)}$$

in the stress space and the plane

$$\sigma_1 + \sigma_2 + \sigma_3 = 0 \quad \text{(EQ 31)}$$

where r is defined by

$$r = \sigma_y \sqrt{\frac{2}{3}} \quad \text{(EQ 32)}$$

Since EQ. 31 is satisfied by strain deviator components, the equation for a von Mises yield surface becomes

$$s_1^2 + s_2^2 + s_3^2 = \frac{2}{3}\sigma_y^2 \quad \text{(EQ 33)}$$

which may also be written as

$$[\sigma_1 - \sigma_2]^2 + [\sigma_2 - \sigma_3]^2 + [\sigma_3 - \sigma_1]^2 = 2\sigma_y^2 \quad \text{(EQ 34)}$$

Furthermore, written in terms of the stress deviator invariant, the yield surface becomes

$$\sigma_y = \sqrt{3J_2}. \quad \text{(EQ 35)}$$

Therefore, the von Mises yield condition is based on the stress deviator and thus are essentially independent of the hydrostatic pressure. This is appropriate for ductile materials, but is not adequate enough to describe all isotropic materials, specifically materials which are dependent on the hydrostatic pressure and the third stress invariant, such as plain concrete and sand.

If a third invariant is included, the circles used to describe the yield condition on the deviatoric plane for the von Mises surface, can become triangular curves with smooth corners. Based on experimental results of concrete, the intersection with the deviatoric plane is triangular at low pressures and circular at higher pressures (see Figure 7).

A model was proposed by William and Warnke, which yields a smooth, convex triangular surface (see Figure 7). If r_c is the coordinate of the surface at the compressive meridian, and r_t the one at the tensile meridian, any intermediate position r may be calculated as follows:

$$r = \frac{2r_c(r_c^2 - r_t^2)\cos\theta + r_c(2r_t - r_c)\sqrt{4(r_c^2 - r_t^2)(\cos\theta)^2 + 5r_t^2 - 4r_t r_c}}{4(r_c^2 - r_t^2)(\cos\theta)^2 + (r_c - 2r_t)^2} \quad \text{(EQ 36)}$$

By dividing both sides by r_c and dividing the numerator and denominator of the right hand side by r_c^2, the equation now becomes

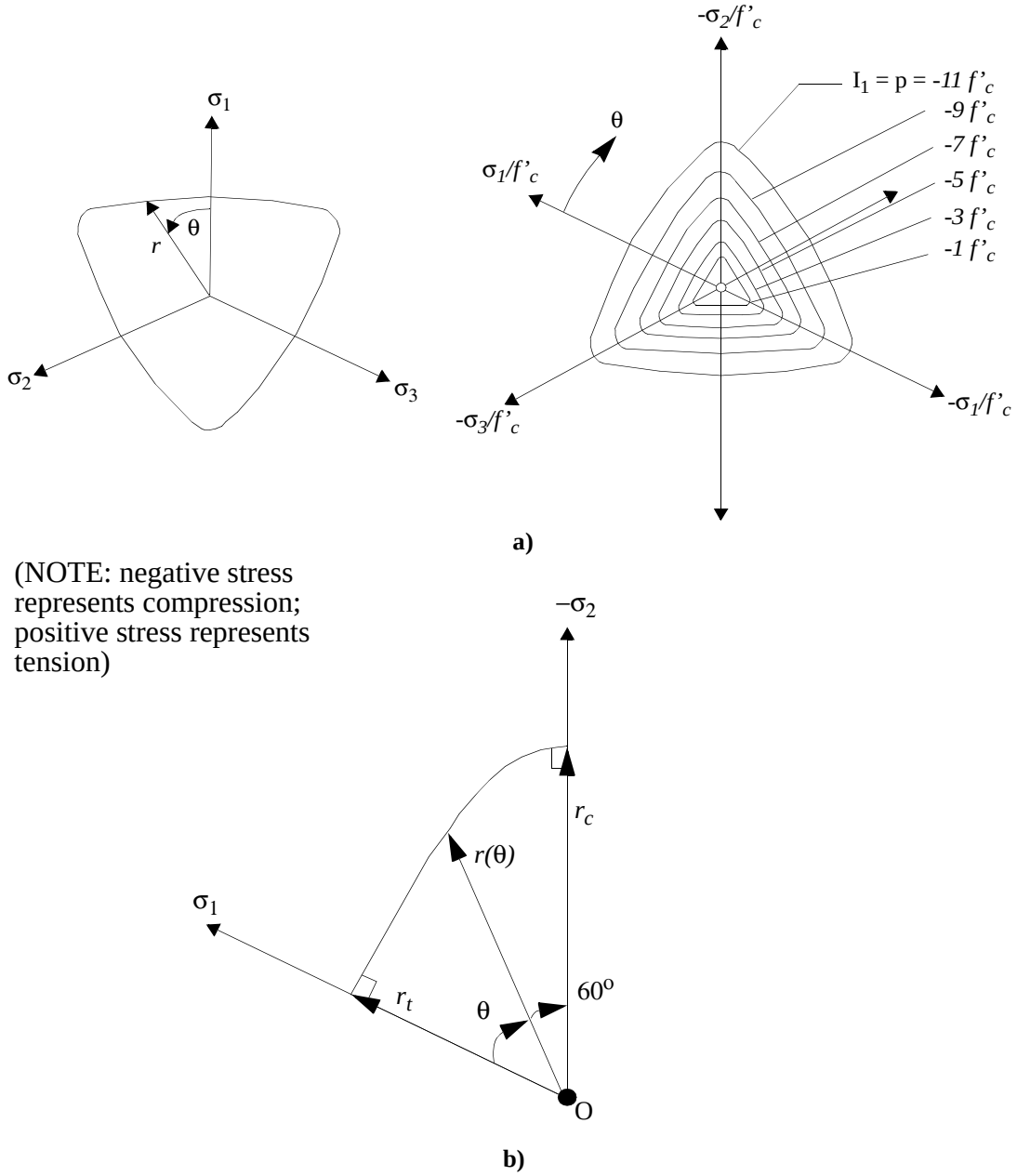

FIGURE 7. a) Concrete deviatoric sections for increasing pressure; b) William and Warnke model.

$$r' = \frac{2(1-\psi^2)\cos\theta + (2\psi-1)\sqrt{4(1-\psi^2)(\cos\theta)^2 + 5\psi^2 - 4\psi}}{4(1-\psi^2)(\cos\theta)^2 + (1-2\psi)^2} \qquad \text{(EQ 37)}$$

where $\psi = r_t / r_c$ and $r' = r / r_c$. Note the similarity between our definition ψ here and the one defined by EQ. 12. For $\theta = 0°$, the formula yields $r' = \psi$, and for $\theta = 60°$ it yields $r' = 1$, where the value of θ can be obtained from the following relationships,

$$\cos\theta = \frac{\sqrt{3}}{2}\frac{s_1}{\sqrt{J_2}} \qquad \text{or} \qquad \cos 3\theta = \frac{3\sqrt{3}}{2}\frac{J_3}{J_2^{3/2}} \tag{EQ 38}$$

Once the value of r' is known, the original compressive meridians are multiplied by r' at that location. By doing this, we obtain separate tensile meridians and compressive meridians as was shown in Figure 2.

Up to this point, it has been said that the compressive meridian is known and the tensile meridian is found by multiplying the compressive meridian by ψ. However, the actual material model, in certain regions, uses the tensile meridian to determine the compressive one. For pressures greater than $f'_c/3$, the input compressive meridians are based on the input parameters a_o, a_1, and a_2, as already stated. For pressures below $f'_c/3$ and above $-f_t$, the tensile meridian is given by

$$\Delta\sigma = \frac{3}{2}(p + f_t) \tag{EQ 39}$$

which passes through both the triaxial tensile test failure point and the uniaxial tensile test point (See “Pressure Cutoff” on page 30.) At $p = f'_c/3$, the two meridians are forced to coincide by determining an appropriate value of ψ. The compressive meridian for pressures below $f'_c/3$ then follows as the image of the tensile meridian, which can be calculated by dividing the tensile meridian by $\psi(p)$ at every pressure p. The determination of $\psi(p)$ is fully discussed in [Ref 2], and will not be discussed in this report. However, it will suffice it to say that the function $\psi(p)$ is determined from experimental data, and are used internally by the code. Therefore, no input is required from the user.

2.5 Strain Rate Effects

In the analysis of concrete structures subjected to blast loading, the concrete may be subjected to strain rates on the order of $10s^{-1}$ to $1000s^{-1}$. At these high strain rates, the apparent strength of concrete and the corresponding strain at peak stress both increase. The fracture energy, or the area under the tensile load-deflection curve, is also believed to increase. Since concrete strain rate effects are generally thought to be dependent on the rate of crack propagation, the elastic modulus is assumed to be rate independent, because at low stress levels no cracking is present. It has been shown by experimental tests that there are different rate enhancements for tensile and compressive loading (see Figure 8). The tensile strength increases by a larger factor than does the compressive strength. Fur-

thermore, the tensile strength rate enhancements have a larger slope than the compressive strength rate effects.

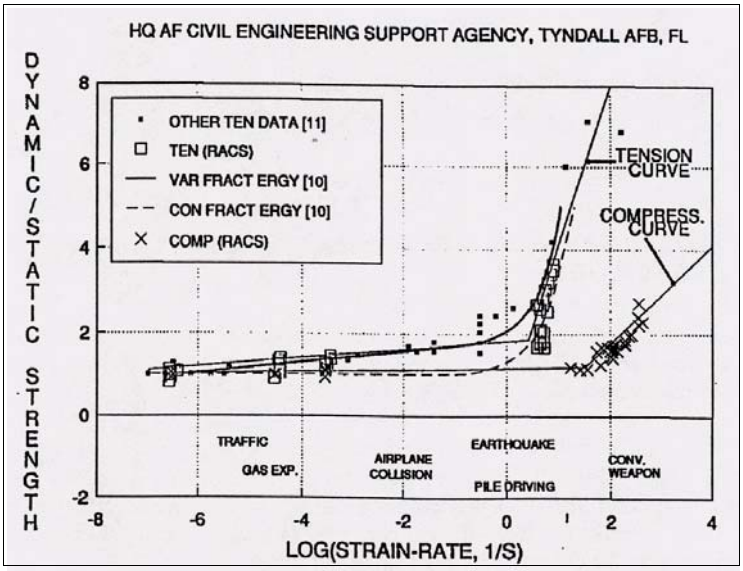

TABLE 2. DYNA3D input

Strain Rate	Strength Factor
-1.000E+02	7.960E+00
-1.000E+01	4.040E+00
-1.000E+00	1.890E+00
-1.000E-01	1.780E+00
-1.000E-02	1.670E+00
-1.000E-03	1.560E+00
0.000E+00	1.000E+00
1.000E-03	1.119E+00
1.000E-02	1.150E+00
1.000E-01	1.200E+00
1.000E+00	1.300E+00
1.000E+01	1.375E+00
1.000E+02	2.000E+00
1.000E+03	3.000E+00

FIGURE 8. Strain rate effects on tensile and compressive strengths ([Ref 3] and [Ref 4]).

The DYNA3D model has the capability of using different strain rate enhancement factors for tension and compression. These factors are input into a DYNA3D via the use of a load curve (see Table 2). Please note that if strain rate effects are to be included in the calculation properly, one must specify a load curve number and also use $s = 100$ on card 4 of the material deck. In addition, the negative values tell the code that those strength factors are to be used for tensile strength, while the positive ones are to be used for compressive strength.

The material model uses the negative values if $p < f_t/3$ and the positive values if $p > f'_c/3$. For pressures that lie between these values, a linear interpolation is used. The rate effects are calculated by obtaining an enhanced $\Delta\sigma_e$ of the failure surface at some pressure p . This calculation is represented by the following:

$$\Delta\sigma_e = r_f \Delta\sigma\left(\frac{p}{r_f}\right) \qquad \text{(EQ 40)}$$

r_f = rate enhancement factor; p = pressure calculated by EOS

First, an unenhanced pressure, p/r_f , is calculated. This allows the code to obtain an unenhanced strength at $\Delta\sigma(p/r_f)$ from the compressive meridians. Then the unenhanced

strength is multiplied by the strength factor to give the enhanced failure surface. This is graphically represented by Figure 9.

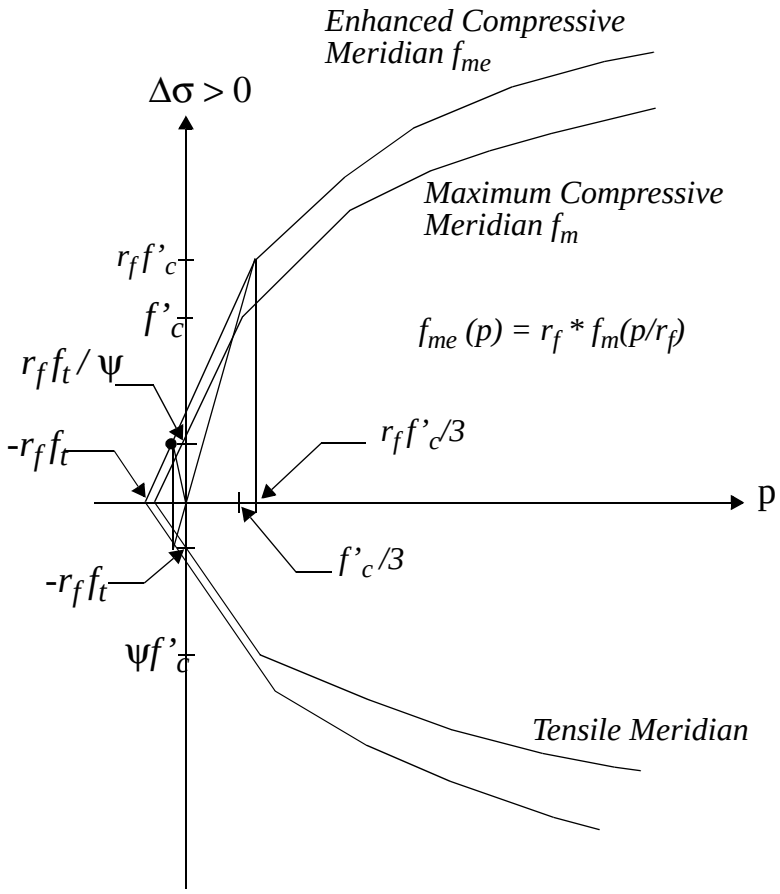

FIGURE 9. Description of strength enhancement calculation.

2.6 Shear Dilation

Dilatancy is a term used to describe the volume increase which may result from the formation and growth of cracks parallel to the direction of the greatest compressive stress. Shear dilation is the volume increase which may occur when concrete is subjected to shear stresses (see Figure 10). When the material is cracking, the dilation continues until the crack opening is large enough to clear the aggregates. At this point, dilatancy does not continue.

To include the effects of shear dilatancy and to make sure that too much shear dilation does not occur, a proper flow rule must be used. As you may recall, in a simple von Mises isotropic hardening law for metals, the plastic flow develops along the normal to the yield surface. This is known as an associative flow rule. If an associative flow rule is used for the concrete model, too much shear dilation tends to occur. In DYNA3D material model 16, the original version of this model, instead used a constant volume Prandtl- Reuss model, which is a non-associative flow rule. This rule, however, has the drawback of not

being able to represent any shear dilation. Therefore, a partial associative flow rule is used, where the amount of associativity is prescribed by the user input value ω, where a value of 0 indicates no change in volume during plastic flow and a value of 1 indicates shear dilation occurs according to an associative flow rule (see Figure 10). Typical concrete experiments show that the value of ω should range from 0.5 to 0.7.

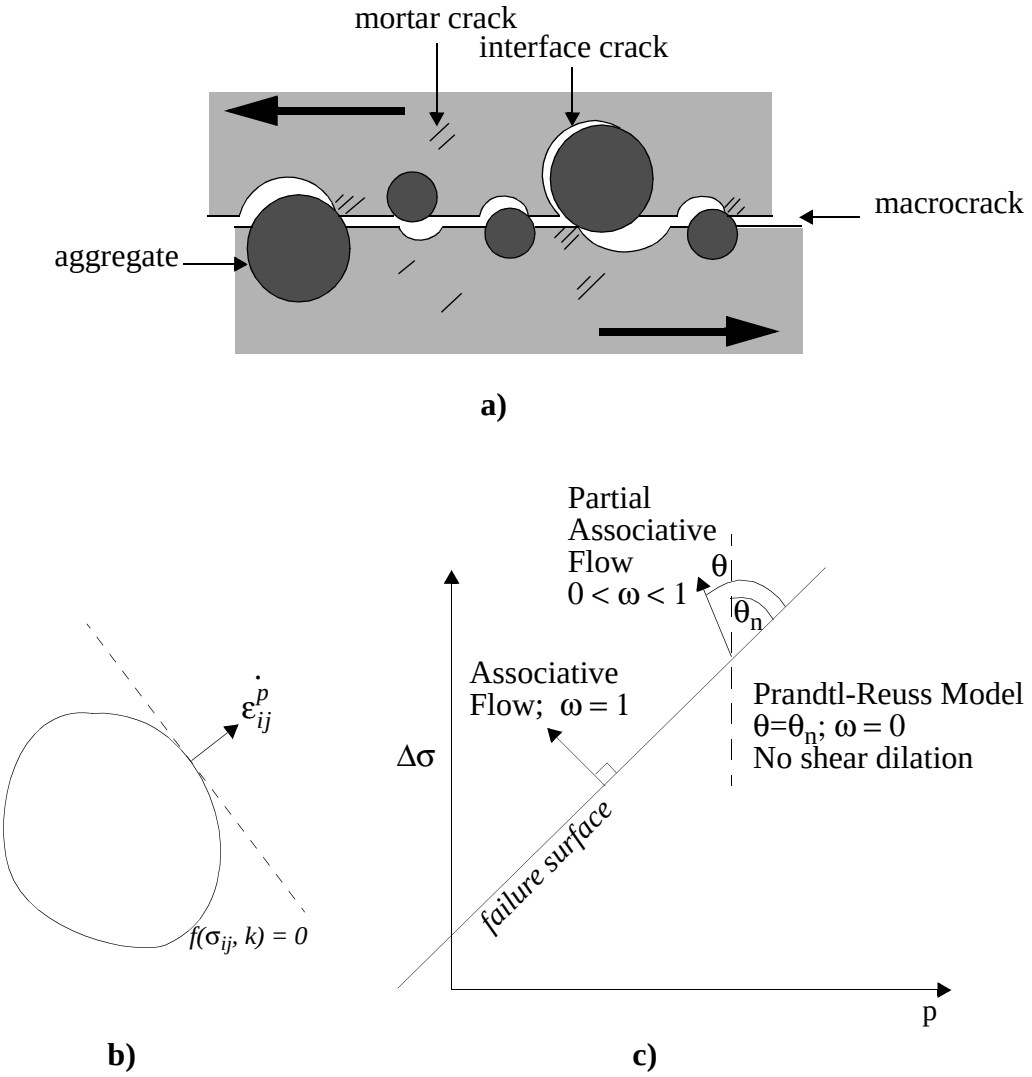

FIGURE 10. a)graphical representation of shear dilation; b) yield surface with associated flow rule; c) description of associative, non-associative, and partial associative flow rules.

2.7 Equation of State

The DYNA3D equation of state form 8 (similarly form 12), prescribes the relationship between pressure and volumetric strain. In addition, it also includes a tabulation of the unloading bulk modulus at peak volumetric strains. Please note that volumetric strain is positive in tension, and pressure is positive in compression. In general, the pressure vs.

volumetric strain may have a cubic spline representation; however, the concrete data that will be supplied in this report consist of a linear pressure vs. volumetric strain relationship see Figure 11, Table 3, and Table 4).

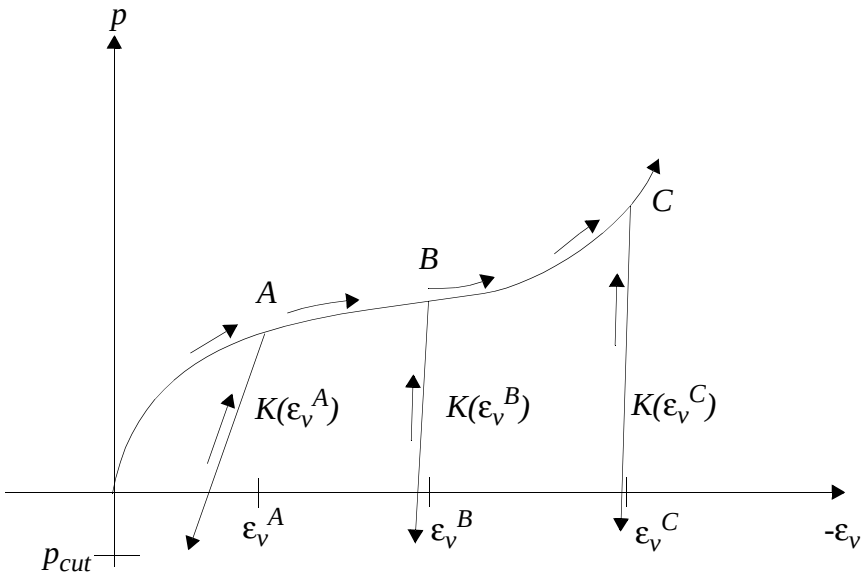

FIGURE 11. Pressure vs. volumetric strain curve for equation-of-state Form 8 with compaction (similarly Form 12).

TABLE 3. Input for equation-of-state form 12: WSMR-5 3/4 concrete

COLUMN 1	COLUMN 2	COLUMN 3	COLUMN 4	COLUMN 5
0.000000000E+00	-1.466000000E-03	-1.000000000E-02	-4.000000000E-02	-7.000000000E-02
-1.000000000E+00	0.000000000E+00	0.000000000E+00	0.000000000E+00	0.000000000E+00
0.000000000E+00	3.625000000E+03	1.513800000E+04	4.437000000E+04	8.076500000E+04
1.032110000E+06	0.000000000E+00	0.000000000E+00	0.000000000E+00	0.000000000E+00
0.000000000E+00	0.000000000E+00	0.000000000E+00	0.000000000E+00	0.000000000E+00
0.000000000E+00	0.000000000E+00	0.000000000E+00	0.000000000E+00	0.000000000E+00
2.472250000E+06	2.472250000E+06	4.437000000E+06	4.437000000E+06	4.437000000E+06
4.437000000E+06	0.000000000E+00	0.000000000E+00	0.000000000E+00	0.000000000E+00
0.000000000E+00	0.000000000E+00	0.000000000E+00	0.000000000E+00	0.000000000E+00

TABLE 4. Input for equation-of-state form 12: SAC5 concrete

COLUMN 1	COLUMN 2	COLUMN 3	COLUMN 4	COLUMN 5
0.000000000E+00	-4.760000000e-03	-1.004760000e+00	0.000000000e+00	0.000000000e+00
0.000000000e+00	0.000000000E+00	0.000000000E+00	0.000000000E+00	0.000000000E+00
0.000000000E+00	1.015000000e+04	7.351500000e+05	0.000000000E+00	0.000000000E+00

TABLE 4. Input for equation-of-state form 12: SAC5 concrete

0.000000000E+00	0.000000000E+00	0.000000000E+00	0.000000000E+00	0.000000000E+00
0.000000000E+00	0.000000000E+00	0.000000000E+00	0.000000000E+00	0.000000000E+00
0.000000000E+00	0.000000000E+00	0.000000000E+00	0.000000000E+00	0.000000000E+00
2.131500000e+06	2.131500000e+06	2.131500000e+06	0.000000000e+00	0.000000000e+00
0.000000000e+00	0.000000000E+00	0.000000000E+00	0.000000000E+00	0.000000000E+00
0.000000000E+00	0.000000000E+00	1.000000000E+00	0.000000000E+00	0.000000000E+00

3.0 Concrete Material Properties

There are two concrete materials which have been used extensively with the DYNA3D material model. These materials include the WSMR-5 3/4 concrete and the SAC5 concrete. Because having only two sets of material data is rather limiting to the user, a procedure for scaling known data to another material is also presented.

3.1 WSMR-5 3/4 Concrete

This material model was used primarily for all of the Morrow Point Dam simulations presented. The primary reason for this is that the unconfined compressive strength of WSMR-5 3/4 concrete is approximately 6500 psi, which is similar to the compressive strength of the cylinder tests conducted on the Morrow Point concrete. The corresponding tensile

strength of this material is approximately 465 psi. Figure 12 shows a plot of the compressive meridians, a single element tensile test, and a uniaxial unconfined compressive test.

3.2 SAC5 Concrete

The SAC5 concrete material was used for the DYNA3D/ALE3D concrete wall benchmark experiment presented earlier in the report. This material has an unconfined compressive strength of approximately 5500 psi and a tensile strength of 365 psi. Furthermore, a comparison of the (η, λ) pairs of SAC5 concrete to those of WSMR-5 3/4 concrete, reveals that the failure surface of SAC5 concrete is reached at a later damage value λ than for the WSMR-5 3/4 concrete. Figure 13 similarly shows a plot of the failure surfaces, a single element tensile test, and a uniaxial unconfined compressive test.

TABLE 5. DYNA3D input for WSMR-5 3/4 concrete: mesh size (6 x 6 x 6 in. cube)

CARDS	COLUMN 1	COLUMN 2	COLUMN 3	COLUMN 4	COLUMN 5	COLUMN 6	COLUMN 7	COLUMN 8
3	1.900E-01	4.640E+02	1.946E+03	4.463E-01	1.228E-05	1.500E+00	5.000E-01	4.417E-01
4	s=0 or 100	2.000E+00	0.000E+00	volumetric strain at failure	0.000E+00	load curve giving rate sensitivity	0.000E+00	0.000E+00
5	0.000E+00	1.000E-05	3.000E-05	5.000E-05	7.000E-05	9.000E-05	1.100E-04	2.700E-04
6	5.800E-04	7.800E-04	1.331E-02	5.000E-01	6.000E-01	1.150E+00	1.469E+03	6.250E-01
7	0.000E+00	8.500E-01	9.600E-01	9.900E-01	1.000E+00	9.900E-01	9.600E-01	5.000E-01
8	5.000E-02	1.000E-02	0.000E+00	0.000E+00	0.000E+00	1.600E-01	1.797E-05	3.981E-05

NOTE: all units in lbs, sec, in.

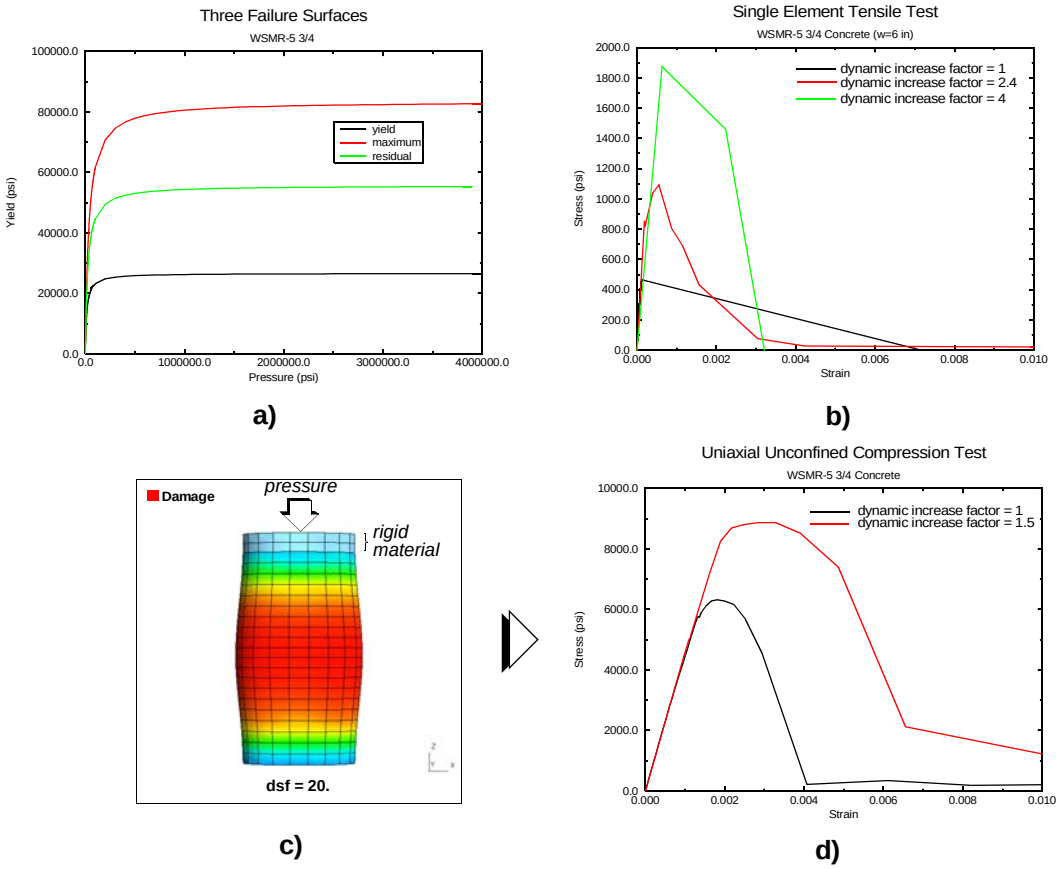

FIGURE 12. WSMR-5 3/4 concrete properties: a) plot of compressive meridians; b) single element uniaxial tensile test with and without rate dependence (tensile strength = 464 psi); c) description of unconfined uniaxial compressive test and plot of damage parameter δ after compressive failure; d) stress-strain plot of UUC test with and without rate dependence (compressive strength = 6500 psi).

TABLE 6. DYNA3D input for SAC5 concrete: mesh size (6 x 6 x 6 in. cube)

CARDS	COLUMN 1	COLUMN 2	COLUMN 3	COLUMN 4	COLUMN 5	COLUMN 6	COLUMN 7	COLUMN 8
3	1.900E-01	3.625E+02	2.192E+03	4.910E-01	1.246E-05	1.400E+00	0.000E+00	4.417E-01
4	s=0 or 100	2.000E+00	0.000E+00	volumetric strain at failure	0.000E+00	load curve giving rate sensitivity	0.000E+00	0.000E+00
5	0.000E+00	1.500E-04	2.800E-04	1.200E-03	0.100E+00	0.200E+00	0.300E+00	0.400E+00
6	5.000E-01	6.000E-01	7.000E-01	8.000E-01	9.000E-01	0.400E+00	1.560E+03	7.414E-01
7	0.000E+00	1.000E+00	2.400E-01	0.000E+00	0.000E+00	0.000E+00	0.000E+00	0.000E+00
8	0.000E+00	0.000E+00	0.000E+00	0.000E+00	0.000E+00	1.500E+00	1.797E-05	3.569E-05

NOTE: all units in lbs, sec, in.

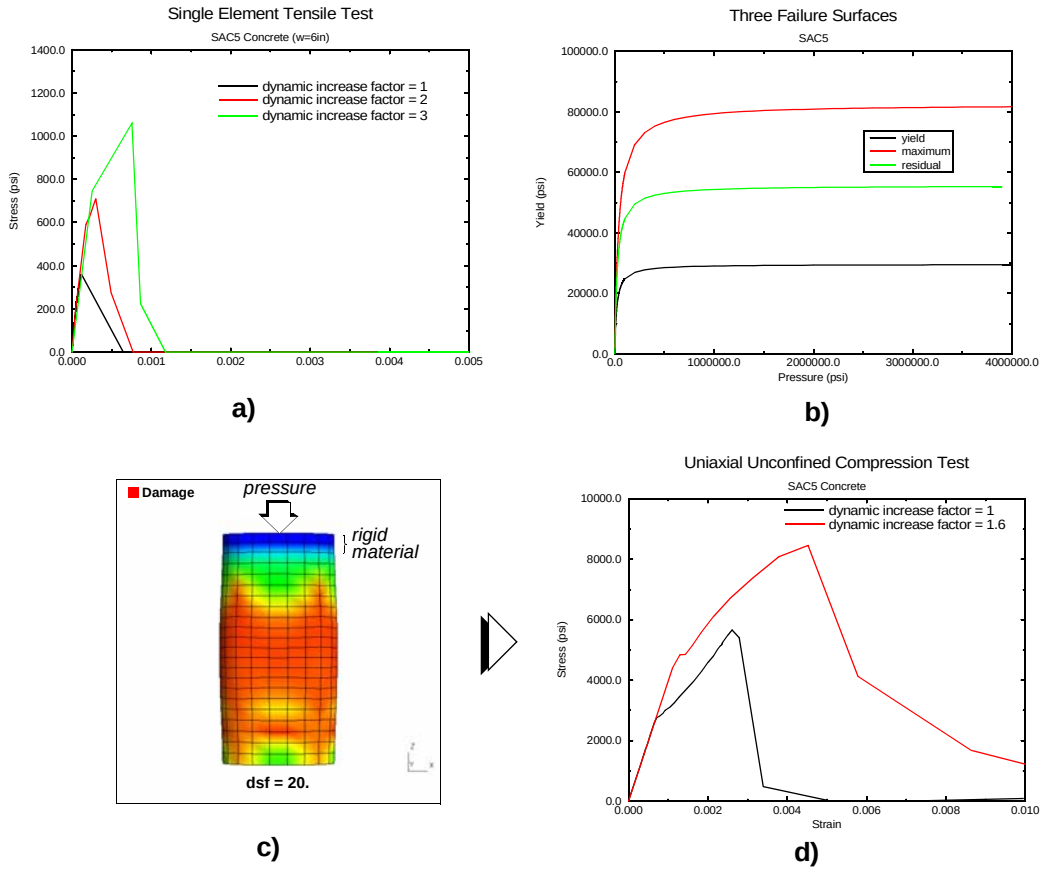

FIGURE 13. SAC5 concrete properties: a) plot of compressive meridians; b) single element uniaxial tensile test with and without rate dependence (tensile strength = 363 psi); c) description of unconfined uniaxial compressive test and plot of damage parameter δ after compressive failure; d) stress-strain plot of UUC test with and without rate dependence (compressive strength = 5500 psi).

3.3 Scaling of Existing Data

A disadvantage to using this particular material model is the large amount of data that is required for one type of concrete. Therefore, it is useful to discuss briefly the methods required to scale the known data, such as the data given for WSMR-5 3/4 concrete and SAC5 concrete, so that it can be used for a different material [Ref 3]. The user input that requires scaling are the failure surfaces and the equation of state.

The following steps are used to scale the failure surfaces:

1. If $f'_{c_{new}}$ is the unconfined compression strength of the new material to be modeled, and $f'_{c_{old}}$ is the unconfined compression strength of a previous modeled concrete material, then a ratio, r, may be calculated as

$$r = \frac{f'_{c_{new}}}{f'_{c_{old}}} \quad \text{(EQ 41)}$$

2. New coefficients for the failure surfaces may be calculated by

$$\begin{aligned} a_{0n} &= a_0 r \\ a_{1n} &= a_1 \\ a_{2n} &= a_2 / r \end{aligned} \quad \text{(EQ 42)}$$

where the subscript n represents the new material's coefficients.

The equation of state needs modification to both the input pressures and input bulk moduli. The new pressures and moduli may be calculated by the two following relationships:

$$p_{new} = p_{old}\sqrt{r} \quad \text{(EQ 43)}$$

$$K_{new} = K_{old}\sqrt{r} \quad \text{(EQ 44)}$$

These relationships stem from the fact that the bulk modulus is calculated by

$$K = \frac{E}{3(1-2\upsilon)} \quad \text{(EQ 45)}$$

where the modulus of elasticity, E, is related to the unconfinced concrete compressive strength by

$$E = 57000\sqrt{f'_c}\ . \quad \text{(EQ 46)}$$

Please note that the empirical relationship for E requires that the units be in (lbs, sec, in).

4.0 References

1. Attaway, S.W., Matalucci, R.V., Morrill, K.B., Malvar, L.J., and Crawford, J.E., Enhancements to PRONTO3D to Predict Structural Response to Blast, Sandia National Laboratories Draft Copy, October 15, 1999.
2. Malvar, L.J., Crawford, J.E., Wesevich, J.W., A New Concrete Material Model For DYNA3D, Karagozian and Case, Report No. TR-94-14.1, June 1, 1994.
3. Malvar, L.J., Crawford, J.E., Wesevich, J.W., A New Concrete Material Model For DYNA3D Release II: Shear Dilation and Directional Rate Enhancements, Karagozian and Case, Report No. TR-96-2.2, February 8, 1996.
4. Ross, C.A., Kuennen, S.T., Tedesco, J.W., "Effects of Strain Rate on Concrete Strength," Session on Concrete Research in the Federal Government, ACI Spring Convention, Washington, D.C., March 1992.

5. Whirley, R.G., DYNA3D: A Nonlinear, Explicit, Three-Dimensional Finite Element Code for Solid and Structural Mechanics, Lawrence Livermore National Laboratory Report UCRL-MA-107254-REV-1.